Translated from *Uspekhi Khimii*, 53, 487-517 (1984) U.D.C. 541.515

The Structure and Stereochemistry of Paramagnetic Metal Complexes of *o*-Quinones

M.I. Kabachnik, N.N.Bubnov, S.P.Solodovnikov, and A.I.Prokof'ev

Data are presented on the EPR spectra of transition metal and Group IV metal complexes with *o*-semiquinone ligands. Analysis of the *g*-factors and the hyperfine coupling constants has been used to determine the structure of the complexes, the electronic configuration of the metal, and the ligand substitution processes.
The bibliography includes 56 references.

CONTENTS

I. Introduction 288
II. The electronic structure of paramagnetic manganese, rhenium, iron, molybdenum, tungsten, and chromium complexes of *o*-quinones 289
III. The stereochemistry of paramagnetic chelate complexes of Group IV elements with semiquinone ligands 299

I. INTRODUCTION

A new branch of the coordination chemistry of metals, associated with the extensive employment of *o*-quinone ligands, has arisen recently. As a result of the characteristic feature of the electronic structure of *o*-quinones, these ligands can function, depending on the conditions, as paramagnetic radical-anions, or diamagnetic catacholate dianions, or, in rare cases, as non-reduced *o*-quinone molecules. Thus, in contrast to the traditional task of coordination chemistry involving primarily the description of the electronic structure of the central metal ion, an additional task involving the determination of the degree of reduction of the ligand arises.

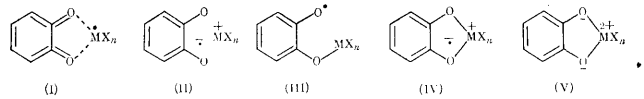
The interest in these systems at the present time is due to the exceptional wide variety of the electronic structures arising in such complexes. However, it was soon discovered that the complexes of *o*-quinones with certain transition metals are biochemically important. It was established that certain micro-organisms employ special substances—"siderophores"—as iron-binding agents.

One of these "siderophores", namely enterobactin, contains in its molecule three catechol groups joined via a macroring. The iron(III) complexes of enterobactin are exceptionally stable[1,2]. It is known that the conditions governing the growth of pathogenic bacteria are definitely related to the iron content in the human organism[3]. Thus the study of the formation and structure of variable-valence metal complexes of *o*-quinones has assumed practical importance.

Numerous studies of the structure of transition metal complexes of *o*-quinones by X-ray diffraction have been analysed in a review[4]. According to the latter[4], the length of the carbonyl bond C—O in the *o*-quinone is a characteristic quantity and makes it possible to estimate the degree of reduction of the ligand. The greatest number of stability constants of the complexes have been determined for the iron(III) ion. It was found that the iron(III) complex of enterobactin has the highest stability constant[5]. It was shown that the synthetic analogues of enterobactin and also of *o*-quinone, having a simple structure, form with Fe^{3+} complexes having high stability constants[5]. The chemical characteristics of transition metal complexes of *o*-quinones include their ability to undergo multistage oxidation and reduction with retention of their structure[4]. It can be assumed that donor—acceptor interactions constitute the basis of the reactions of these complexes with N_2, CO, and O_2. It has been found that the vanadium complexes of catechol actively fix molecular nitrogen under certain conditions[6]. The vanadium complexes also proved capable of reversible combination with O_2, NO, and CO.[7]

The formal examination of the electronic structure of metal complexes of *o*-quinones is usually carried out within the framework of the oxidation-reduction triad of the *o*-quinone. Taking into account the coordination, it is possible to postulate different structures of the complex of *o*-quinone with the organometallic fragment $\dot{M}X_n$ having an odd number of electrons. We shall consider paramagnetic complexes of precisely this type.

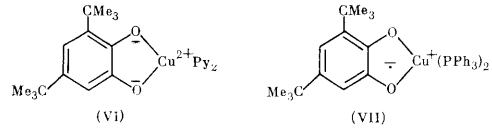
In principle, the *o*-quinone ligands can give rise to the following types of complexes:



(I) (II) (III) (IV) (V)

The formation of a particular structure depends on the nature of M and X and on the number *n*. Structure (I) corresponds to the coordination of the neutral *o*-quinone via the unshared electron pairs of the oxygen atoms. Structures (II)—(IV) correspond to the coordination of the semi-reduced form of the quinone—the semiquinone radical-anion—and differ in the distribution of the unpaired electron between the metal and the ligand. Structure (V) reflects the coordination of the fully reduced quinone—the catecholate dianion.

The change in the degree of oxidation of the copper atom and of the degree of reduction of the ligand in the following complexes can serve as a clear example of the transformation of the structures[8,9]:



(VI) (VII)

The energy differences between structures (VI) and (VII) are small and the replacement of pyridine by triphenylphosphine leads to a sharp alteration of the electronic structure of the complex. In certain cases the possibility of equilibrium between forms (VI) and (VII) has been postulated,

as, for example, in the case of the bipyridyl adduct of the cobalt complex of 3,5-di-t-butyl-*o*-benzoquinone.[10] However, such hypotheses must be accompanied by an indication of the character of the skeletal changes in the complexes without which no transitions between the "electronic isomers" are of course possible. A convenient method for the investigation of the above transitions involves the photochemical synthesis of the complexes of *o*-quinones with radical organometallic fragments. In contrast to other methods[11–14], it makes it possible to determine not only the final reaction products but also the unstable intermediate complexes.

The coordination chemistry of Group IV elements has developed to a much lesser extent than that of transition metals. The employment of semiquinone paramagnetic ligands leads to new possibilities for the study of the stereochemistry of the coordination compounds of silicon and tin. Electron paramagnetic resonance (EPR) and electronic absorption spectroscopy have been used as the main procedures for the investigation of the electronic structure of the *o*-quinone complexes.

The aim of the present review was to examine the characteristics of the structures of the complexes and the wide variety of the electronic configurations of the metal and the ligands and to demonstrate the possibilities of the EPR method from the standpoint of the solution of various stereochemical problems.

II. THE ELECTRONIC STRUCTURE OF PARAMAGNETIC MANGANESE, RHENIUM, IRON, MOLYBDENUM, TUNGSTEN, AND CHROMIUM COMPLEXES OF *o*-QUINONES

1. The EPR and Electronic Absorption Spectra of the Complexes of *o*-Quinones with Manganese and Rhenium Penta- and Tetra-carbonyls

It is known that the photolysis of manganese and rhenium decarbonyls leads to the formation of the corresponding radicals[13]:

$$(CO)_5M—M(CO)_5 \xrightarrow{h\nu} 2\dot{M}(CO)_5,$$

where M = Mn or Re. The interaction of these radicals with *o*-quinones leads to the formation of complexes having different structures depending on the temperature.

When manganese pentacarbonyl was allowed to react with *o*-quinones, it was possible to detect primary radicals which had not been found in previous studies[16–19], to determine their stabilities, and to measure the rate constants for their reactions[22]. The photolysis of $M_2(CO)_{10}$ in the presence of 3,6-di-t-butyl-*o*-benzoquinone and pentane at −80 °C leads to the appearance of a radical whose EPR spectrum corresponds to the interaction of the electron with the ^{55}Mn ($I = 5/2$) nucleus and with the two non-equivalent protons of the catechol ligand (Fig.1).

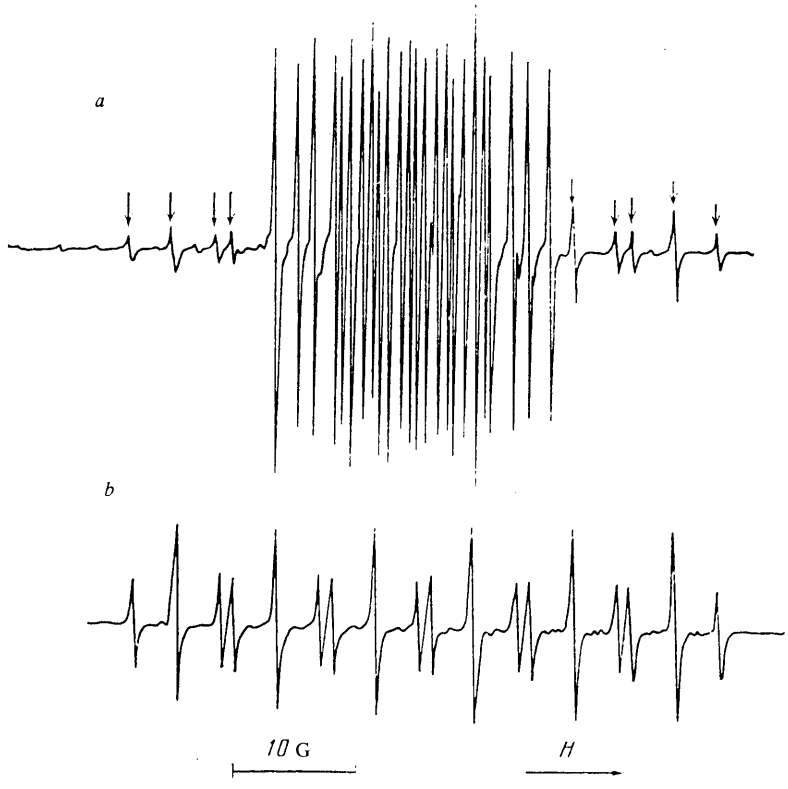
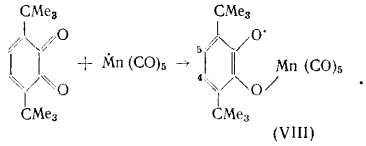


Figure 1. EPR spectra of the radicals (VIII) (*a*) and (IX) (*b*) in pentane at −80 °C (*a*) and 20 °C (*b*); the arrows indicate the lines of the radical (IX).[22]

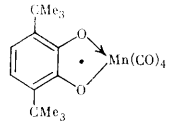
On the basis of the characteristics of the distribution of the unpaired electron density in the catechol ligand, a structure with the unpaired electron localised at the oxygen atom was attributed to the radical (VIII):



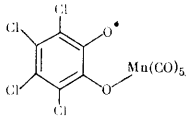
(VIII)

The larger hyperfine coupling contant (HFC) (5 G) is attributed to the ring proton in the 4-position relative to the univalent oxygen atom of the catechol ligand and the smaller constant (1.7 G) is attributed to the proton in the 5-position. In the temperature range from −100° to 20 °C, the alternation of the hyperfine structure (HFS) line widths is not manifested in the EPR spectra of the complex (VIII), which permits the conclusion that the $-M(CO)_5$ fragment does not migrate between the oxygen atoms of the catechol ligand in the radical (VIII) on the EPR time scale. The difficulty of achieving tautomeric transitions in this case is probably associated with the coordination saturation of the manganese atom and with the impossibility of the additional coordination to the latter of the univalent oxygen atom.

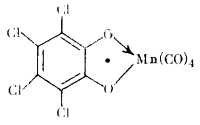
The radical (VIII) is relatively unstable and on heating above −80 °C is converted (in the absence of ultraviolet radiation) into the radical (IX), characterised by appreciable hyperfine coupling with the ^{55}Mn nucleus and with the two equivalent protons of the catechol ligand (Fig.1 and Table 1). Table 1 presents the spectroscopic characteristics of species having the following structures:



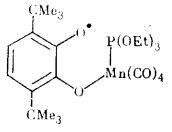
(IX)



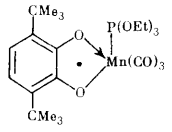
(X)



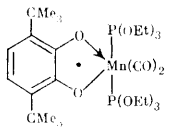
(XI)



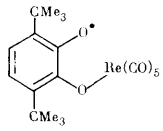
(XII)



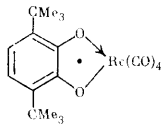
(XIII)



(XIV)

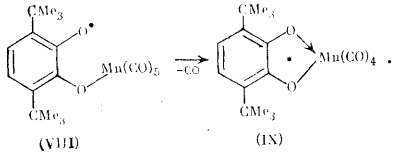


(XV)



(XVI)

Because of the low stability of the radical (VIII), the latter was not detected in previous studies[16-19]. There is controversy concerning the structures of the radicals (IX), namely whether they contain the $Mn(CO)_5$ or $Mn(CO)_4$ fragments. It has been suggested[16,17] that the fragment $Mn(CO)_4$ is present in radicals of type (IX). The data obtained by Tumanskii et al.[22] constitute important evidence in support of this hypothesis and the radical (IX) is probably formed on elimination of one CO group from the primary radical (VIII):



(VIII) (IX)

Table 1. The spectroscopic parameters (G) of the primary and secondary radicals formed on interaction of *o*-quinones with manganese and rhenium pentacarbonyls.[22,23]

Radical	$a_{H(4)}$	$a_{H(5)}$	a_{Mn}	a_P
(VIII)	5.0	1.7	3.0	—
(IX)	3.4	3.4	7.7	—
(X)	—	—	2.8	—
(XI)	—	—	8.7	—
(XII)	5.1	1.7	2.2	6.0
(XIII)	3.15	3.15	10.1	43.0
(XIV)	2.7	2.7	16.1	54.0
(XV)	—	—	6.6	—
(XVI)	3.8	3.8	29.0	—

Note: a_{Cl} = 0.47 G [the average of the constants for the hyperfine coupling of the unpaired electron with the $^{35}Cl(^{37}Cl)$nuclei] was obtained for the radical (XI); the constants for the hyperfine coupling of the unpaired electron with the ^{185}Re and ^{187}Re nuclei are quoted instead of a_{Mn} for the radicals (XV) and (XVI).

To confirm the transformation of the radical (VIII) into the radical (IX), a study was made of the kinetics of the destruction of the radicals (VIII) and of the accumulation of the radicals (IX), the analysis of which indicates the unimolecular character of the conversion of (VIII) into (IX) and the extremely similar rate constants for the destruction of the radicals (VIII) (3.0×10^{-3} s^{-1}) and for the accumulation of the radicals (IX) (3.3×10^{-3} s^{-1}) at −30 °C show that the radical (VIII) is almost entirely converted into the radical (IX). The general expression for the rate constant for the unimolecular conversion of the radical (VIII) into the radical (IX) is[22]

$$k(s^{-1}) = 2 \cdot 10^{15} \exp[-(17300 \pm 1000)/RT]$$

and $k(-20\ °C) = 0.017\ s^{-1}$.

The stability of the primary manganese-containing radicals investigated depends significantly on the structure of the *o*-quinone employed. In the case of *o*-chloranil, the primary radicals (X) (see Table 1), which differ from the secondary radicals (XI) by the constants for the hyperfine coupling with the ^{55}Mn and ^{35}Cl, ^{37}Cl nuclei, proved to be much less stable than the corresponding complexes with the 3,6-di-t-butyl-1,2-dihydroxybenzene ligands. The rate of destruction of the radicals (X) proved to be appreciably higher than the rate of accumulation of the radicals (XI), which shows that, apart from the elimination of the CO group, the primary radicals derived from *o*-chloranil participate also in other destruction processes. However, the activation energies for the destruction of the radicals (X) and the accumulation of the radicals (XI) proved to be approximately identical. The overall expression for the rate constant for

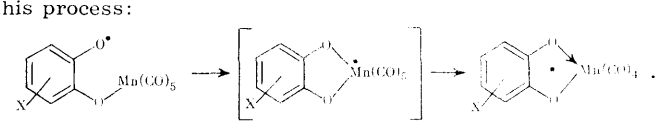
the transformaton of the primary radical (X) into the secondary radical (XI), determined from the curve for the accumulation of the secondary radical (XI), is

$$k(s^{-1}) = 5 \cdot 10^{8} \exp[-(7600 \pm 1000)/RT]\,.$$

Triethyl phosphite (TEP) exerts a significant influence on the stability of the primary radicals. The photolysis of $M_2(CO)_{10}$ in the presence of 3,6-di-t-butyl-*o*-benzoquinone with added TEP leads to the appearance of a primary radical to which the structure (XII) was attributed (Table 1), with an asymmetric distribution of the unpaired electron density in the catechol ligand (this is indicated by the difference between the HFC constants for the ring protons) and with additional hyperfine coupling with the ^{31}P nucleus. The rate of conversion ($k = 0.0013\ s^{-1}$) of the radical (XII) into the secondary radical (XIII), characterised by the equivalent HFC constants for the ring protons and the much higher HFC constant due to the coupling with the ^{31}P nucleus, is appreciably lower than the rate of conversion of the radical (VIII) into the radical (IX) at −20 °C presented above[23].

After prolonged illumination of the reaction mixture in an excess of TEP, yet another CO group is substituted by a TEP molecule in the coordination sphere of manganese, and the radical (XIV), whose spectroscopic characteristics are listed in Table 1, is generated[23].

The large difference between the destruction constants of the primary radicals as a function of the structure of the ligands at the manganese atoms shows that the rate-limiting stage of the process is apparently intramolecular attack on the central manganese atom by the univalent oxygen atom of the catechol ligand. The electron-accepting properties of the ligand and the electron-donating properties of the manganese-containing fragment play an important role in this process:



The primary rhenium complexes (XV) and the secondary rhenium complexes (XVI), formed in the photochemical reacton of 3,6-di-t-butyl-*o*-benzoquinone with $Re_2(CO)_{10}$, have a much greater line width in the EPR spectra, in contrast to the analogous manganese-containing complexes, which leads in some cases to the blurring of the proton hyperfine structure. In the transition from (XV) to (XVI) a sharp increase of the constants for the hyperfine coupling with the ^{185}Re, ^{187}Re nuclei is observed (see Table 1).[23] It follows from Table 1 that the substitution of the CO group by a TEP molecule leads to an appreciable shift of the unpaired electron density from the *o*-quinone ligand to the manganese, rhenium, and phosphorus atoms.

Analysis of the EPR spectrum of the radical (VIII) demonstrates unambiguously the asymmetric addition of the *o*-quinone ligand to $\dot{M}n(CO)_5$. However, it is difficult to estimate the polarity of the bond between the ligand and $\dot{M}n(CO)_5$ from the difference $a_{H(4)} - a_{H(5)}$. To solve this problem, a study was made[20] of the electronic absorption spectra of the test complexes. Fig.2 illustrates the electronic absorption spectra of the manganese complexes (VIII), (IX), (XIII), and (XIV) in pentane. On heating from −100° to 20 °C, it is possible to observe a successive decrease of the intensity of the bands of (VIII) and an increase of the band of (IX). An analogous behaviour has been observed also in the transformation of the rhenium complexes. Table 2 presents the spectroscopic data for the complexes investigated. In the spectra of the complexes (VIII) and (XV), the primary complexes of manganese and rhenium, there are two absorption bands in the visible region: near 600 nm and a more intense band in the range 400–500 nm. The spectra of the complexes (IX) and (XVI), the secondary complexes of manganese and rhenium, contain one band in the visible region. A band in the ultraviolet region with $\lambda_{max} \approx 300$ nm has been observed in the spectrum of a rhenium complex of type (XVI) with the 3,5-di-t-butyl-1,2-dihydroxybenzene ligand. The extinction coefficients of such complexes, determined by Gerber and Wan[21], amount to $\sim 10^3$ litre mole^{-1} cm^{-1}.

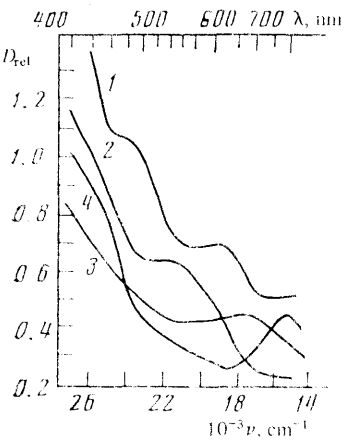


Figure 2. Electronic absorption spectra of manganese complexes in pentane: *1*) (VIII) at −100 °C; *2*) (IX) at 20 °C; *3*) (XIII) at −150 °C; *4*) (XIV) at 20 °C.

Table 2. The frequencies of the $\pi \rightarrow \pi^*$ transitions in the electronic absorption spectra of the *o*-semiquinone complexes of manganese and rhenium carbonyls[20].

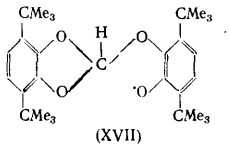
Complex	Solvent	ν, cm^{-1}
$Q^{\cdot-}Mn^{I}(CO)_5$	Toluene	16600; 20800
$Q^{\cdot-}Mn^{I}(CO)_5$	Pentane	16500; 21600
$Q^{\cdot-}Re^{I}(CO)_5$	Toluene	16000; 20800
$Q^{\cdot-}Mn^{I}(CO)_4$	Toluene	17000
$Q^{\cdot-}Mn^{I}(CO)_4$	Pentane	19200
$Q^{\cdot-}Re^{I}(CO)_4$	Toluene	20000
$Q^{\cdot-}Re^{I}(CO)_4$	Pentane	20800
$Q^{\cdot-}Mn^{I}(CO)_3P(OEt)_3$	Pentane	13000
$Q^{\cdot-}Mn^{I}(CO)_2[P(OEt)_3]_2$	Pentane	12500
$Q^{\cdot-}Re^{I}(CO)P(OEt)_3$	Pentane	17200
$Q^{\cdot-}Re^{I}(CO)_2[P(OEt)_3]_2$	Pentane	15000
$Q^{\cdot-}Mn^{I}(CO)_3NBu_3$	Pentane	14500
$Q^{\cdot-}Mn^{I}(CO)_3(CH_3)_2CO$	Acetone	18800 (20 °C), 21 200 (−50 °C)
$Cl_2Q^{\cdot-}Mn^{I}(CO)_4$	Hexane	16000

Notation: Q = .

Successive substitution of two CO groups in the complex (IX) by two TEP molecules[22,23] leads to a strong bathochromic shift of the band at 540 nm (Fig.2). When the reaction is carried out at temperatures between −20° and −15 °C, a band, corresponding to the complex (XIV), appears at 670 nm. On further heating, the 670 nm band disappears.

and a new band with λ_{max} = 800 nm appears; when the reaction is carried out at room temperature, this band appears at once. After the measurement of the spectra of (IX) and (XIV), part of the soluton was transferred to a tube for the investigation of the EPR spectra. The signal splittings due to the interaction with the nuclei of hydrogen, manganese, and phosphorus atoms, observed in the EPR spectra[22,23], confirm the assignment of the bands in the electronic spectra to species having the corresponding structure. Analogous shifts of the long-wavelength absorption band on substitution of the CO groups by TEP take place in the corresponding rhenium complexes (XVI). A bathochromic shift is observed also in the spectra of the complex (VIII) in the presence of tributylamine, which indicates the substitution of the CO group by an amine molecule.

The similarity of the spectroscopic characteristics of the manganese and rhenium complexes (VIII) and (XV) and the complexes (IX) and (XVI) is associated with the similarity of their structures and the fact that the chromophore responsible for their absorption in the visible region is an *o*-semiquinone ligand. Although the electronic absorption spectra of certain *o*-semiquinone radical-anions had been obtained earlier[24-26], the influence of coordination on the positions of the absorption bands had not been investigated. In order to consider the spectra of the manganese and rhenium complexes, a study was made of the influence of the coordination of the Na^+ cation and the *o*-semiquinone ligand on the spectrum of the corresponding sodium *o*-semiquinolate (O^-Na^+) in tetrahydrofuran (THF) and the electronic absorption spectrum of the radical (XVII), in which the catechol ligands are bound covalently to the central carbon atom, was measured:



(XVII)

Fig. 3 illustrates the spectra of Q^-Na^+ at 70° and −70 °C. At −70 °C the 770 nm band shows a shoulder at 660 nm, which disappears on heating and reappears on cooling. According to Prokof'ev[27], the fraction of contact ion pairs in THF increases with decrease of temperature (ΔH = 1.7 ± 0.2 kcal mol^{-1}) and for this reason we assigned the shoulder at 660 nm to two contact ion pairs. Thus the coordination of the ions in Q^-Na^+ leads to an appreciable hypsochromic shift and an increased time of contact between this complex and a sodium mirror results in the decolorisation of the solution associated with the formation of a diamagnetic dianion. The spectrum of the dianion has a single absorption maximum at 305 nm. For comparison, we shall indicate the positions of the absorption band maxima of the corresponding catechol derivative (270 nm) and the orthocarbonic ester of catechol, which is a precursor of the radical (XVII) (270 nm). When air is admitted into the cuvette containing the dianion, the characteristic blue colour of the radical-anion reappears and its spectrum is measured.

The electronic spectrum of the radical (XVII), obtained by oxidising the corresponding phenol with lead dioxide, contains a band with λ_{max} = 400 nm, on which there are two shoulders, at 380 and 420 nm.[20] It follows from these data that, in the presence of a covalent bond at the second oxygen atom, a larger hypsochromic shift of the absorption bands is observed in the spectrum of the radical than that of the bands due to the *o*-semiquinone radical-anion. Comparison of the spectra of the complexes (VIII) and (IX), on the one hand, and those of (XV) and (XVI), on the other, with the spectra of Q^-Na^+ (Fig. 3) demonstrates a great similarity both in the positions of the bands and their intensities. Such similarity indicates a high polarity of the metal–oxygen bond and that the ligand is present in the radical-anionic form[28].

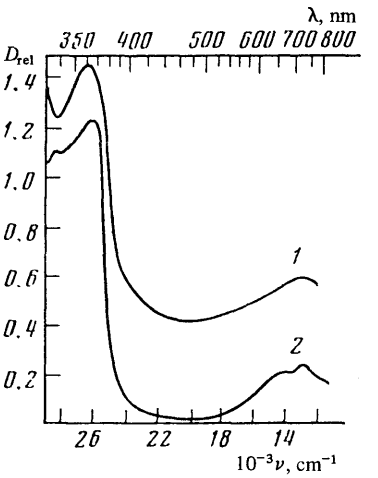


Figure 3. Electronic spectra of the radical-anion $Q^-(Na^+)$ in THF at 70 °C (curve *1*) and −70 °C (curve *2*).[20]

The involvement of the second oxygen atom in the bond with the metal in the complexes (VIII) and (XVI) leads to an appreciable hypsochromic shift of the bands in the absorption spectrum, which may be associated with a definite contribution of a covalent chelate structure, arising as a result of the effective exchange interaction between the d_{xz} and d_{yz} orbitals of the metal and the π electrons of the ligand[20].

2. The EPR Spectra of the *o*-Quinone Complexes of Iron, Molybdenum, and Tungsten Metallocenes

The substitution of the CO groups in iron, molybdenum, and tungsten carbonyls by the cyclopentadienyl ligand leads to an alteration of the even number of *d* electrons of the metal to an odd number, which results in the possibility of the formation of dinuclear complexes. It is believed that the cyclpentadienyl ligand in the dimeric complex $[Mo(CO)_3 . \pi\text{-}C_5H_5]_2$ has a negative charge, is a donor of three electron pairs, and occupies three coordination sites, the molybdenum atom having a formal +1 oxidation state and a coordination number of 7.[29] The photolysis of such dimers leads to the appearance of the corresponding metal-centered radicals, which react with *o*-quinones to form paramagnetic complexes[30].

The EPR spectra of the paramagnetic complexes arising on photolysis of $Fe_2(\pi\text{-}C_5H_5)_2(CO)_4$, $Mo_2(\pi\text{-}C_5H_5)_2(CO)_6$, and $W_2(\pi\text{-}C_5H_5)_2(CO)_6$ in the presence of 3,6-di-t-butyl-*o*-benzoquinone, 3,5-di-t-butyl-*o*-benzoquinone, and *o*-chloranil (3,6-Q, 3,5-Q, and Cl_4Q respectively) have been investigated[43]. The primary paramagnetic products detected in the temperature range −100° to −60 °C in a 2 : 1 pentane–toluene mixture have spectra whose common feature is an asymmetric distribution of spin density in the *o*-quinone ligand [$a_{H(4)} \neq H(5)$], which reflects the non-equivalent involvement of the oxygen atoms in the formation of a bond

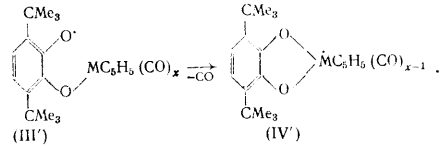
between the ligand and the metal. The HFC constants and the g-factors are listed in Table 3.

Table 3. Parameters of the EPR spectra of the adducts of $FeC_5H_5(CO)_3$ and $WC_5H_5(CO)_3$ with o-quinones[43].

Complex	$a_{H(4)}$, G	$a_{H(5)}$, G	a_M, G	$\tilde{g}$	g_1	g_2	g_3
(III′) 3,6-QFeC$_5$H$_5$(CO)$_2$	4.6	1.5	—	2.001	—	—	—
(III′) 3,5-QFeC$_5$H$_5$(CO)$_2$	—	2.8	—	2.000	—	—	—
(IV′) 3,6-QFeC$_5$H$_5$CO	—	—	—	2.048	2.104	2.033	2.006
(IV′) 3,5-QFeC$_5$H$_5$CO	—	—	—	2.046	—	—	—
(III′) 3,6-QMoC$_5$H$_5$(CO)$_3$	5.3	0.9	—	2.003	—	—	—
(III′) 3,5-QMoC$_5$H$_5$(CO)$_3$	—	2.3	—	2.002	—	—	—
(IV′) 3,6-QMoC$_5$H$_5$(CO)$_2$	1.0	1.0	15.6	1.990	—	—	—
(XIX) (3,6-Q)$_2$MoC$_5$H$_5$	—	—	37.3	1.868	1.989	1.971	1.952
(XIX) (3,5-Q)$_2$MoC$_5$H$_5$	—	—	36.4	1.968	1.990	1.972	1.949
(XIX) (Cl$_4$Q)$_2$MoC$_5$H$_5$	—	—	38.8	1.965	1.991	1.976	1.941
(XIX) 3,6-Q(Cl$_4$Q)MoC$_5$H$_5$	—	—	—	—	1.990	1.975	1.945
(III′) 3,6-QWC$_5$H$_5$(CO)$_3$	6.9	0.8	—	1.999	—	—	—
(III′) 3,5-QWC$_5$H$_5$(CO)$_3$	—	3.8	—	2.001	—	—	—
(XIX) (3,6-Q)$_2$WC$_5$X$_5$	—	—	72.5	1.902	1.960	1.912	1.842
(XIX) 3,6-Q(Cl$_4$Q)WC$_5$H$_5$	—	—	—	—	1.960	1.923	1.824

Note: 3,6-Q = 3,6-di-t-butyl-1,2-dihydroxybenzene ligand; 3,5-Q = 3,5-di-t-butyl-1,2-dihydroxybenzene ligand; Cl$_4$Q = o-chloranil ligand. Compexes of type (III′) all have the structure of phenoxy-radicals, while complexes of type (IV′) have chelate structures with the predominant localisation of the unpaired electron at the metal atom (see text).

In contrast to the complexes of manganese and rhenium pentacarbonyls, the ligand-centered free radicals considered in this section are converted into new metal-centered free radicals (Table 3):



In the case of molybdenum and tungsten, the metal-centered free radicals undergo further changes associated with the substitution of the CO groups by the o-quinone.[43]

The EPR spectra of the liquid and solid solutions of the metal-centered free radicals are presented in Figs.4–6. The change in the g-factor in solution relative to its value for the free electron, the strong anisotropy of the g-factor and the absence of an appreciable hyperfine coupling with the hydrogen atoms of the ligands in solution show that the unpaired electron occupies the 3d(Fe), 4d(Mo), and 5d(W) orbitals of the corresponding metal atoms. Analysis of the EPR spectra of the solid solutions shows that the paramagnetic species are characterised by an overall spin $S = 1/2$ in all cases.

In the radicals of the type $\dot{M}(C_5H_5)(CO)_x$ the iron, molybdenum, and tungsten atoms should have the $3d^7$, $4d^5$, and $5d^5$ configurations respectively. The number of d electrons of the metal atom in the complex depends on the degree of

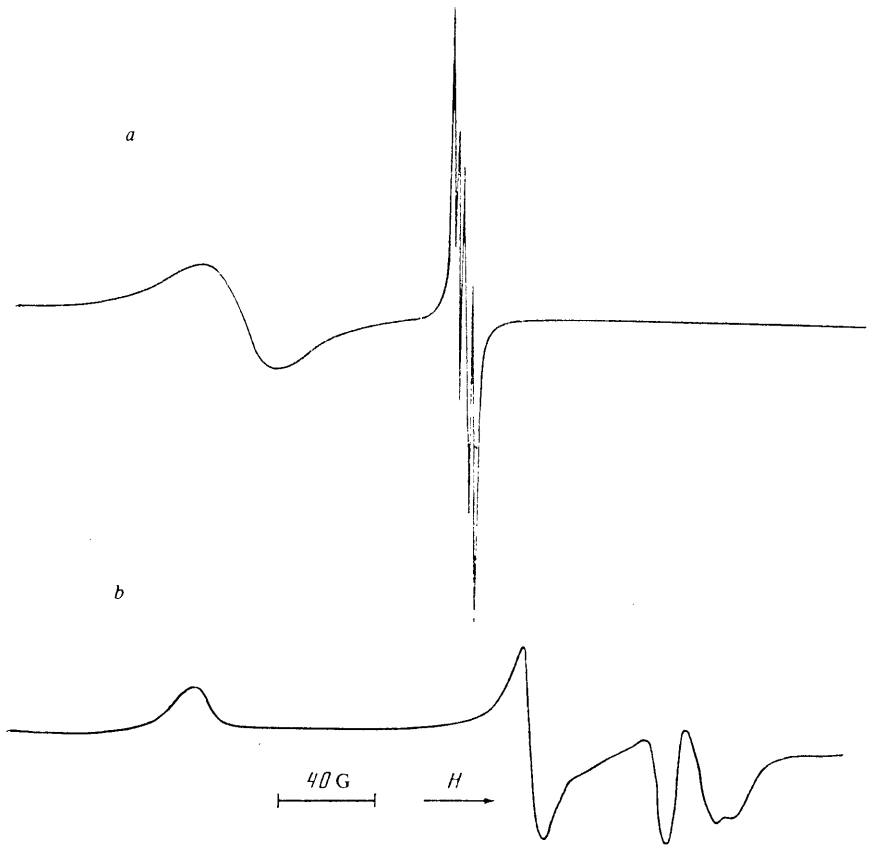


Figure 4. EPR spectra of 3,6-Q$\dot{F}$eC$_6$H$_5$CO: a) solution, −75 °C; b) solid solution, 155 °C.[43]

its oxidation by the *o*-quinone ligands. Depending on the degree of reduction of the *o*-semiquinone ligand (from semiquinone to the catecholate), the metal atom loses one or two electrons. When metal-centered free radicals are formed from $\dot{M}(C_5H_5)(CO)_x$ and *o*-quinones, a bond should be formed either by two electrons of the catecholate anion or by the unshared electron pairs of the oxygen atoms of the carbonyl groups in the non-reduced form of the quinone. The nature of the bond between the *o*-quinone ligands and metals has been investigated by X-ray diffraction[31,32].

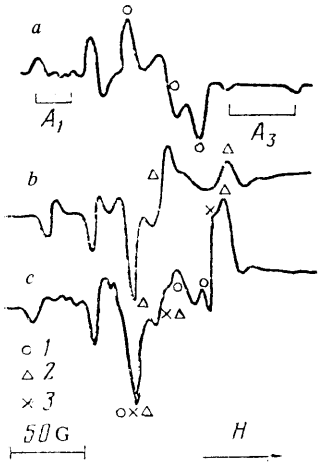
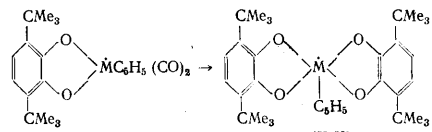


Figure 5. EPR spectra of solid solutions of molybdenum complexes: *a*) $(3,6\text{-Q})_2\dot{M}oC_5H_5$, −150 °C (*1*); *b*) $(Cl_4Q)_2.\dot{M}oC_5H_5$, −155 °C (*2*); *c*) mixture of $(3,6\text{-Q})_2\dot{M}oC_5H_5$ (*1*), $(Cl_4Q)_2MoC_5H_5$ (*2*), and $3,6\text{-QCl}_4\text{Q}\dot{M}oC_5H_5$ (*3*), −150 °C, 3,6-Q/Cl_4Q = 1; A_1 and A_3 are the components of the tensor of the hyperfine coupling with the ^{95}Mo(^{97}Mo) nuclei[43].

For the iron complexes, it is necessary to make a choice between the $3d^7$ and $3d^5$ electronic structures. For the $3d^7$ configuration, the non-reduced *o*-quinone is coordinated, while in the case of the $3d^5$ configuration the complex should have a catecholate linkage. According to Buchanan et al.[31], in the tris-*o*-quinone complexes of iron, all the ligands are reduced to the semiquinone state only. On the basis of these data, one can postulate that in the metal-centered complexes of 3,6-Q and 3,5-Q with $Fe(C_5H_5)(CO)_2$ the non-reduced form of the *o*-quinone is coordinated. It is of interest that the replacement of 3,6-Q and 3,5-Q by *o*-chloranil (Cl_4Q), which has more pronounced electron-accepting properties, leads solely to ligand-centered radicals characterised by a *g*-factor close to 2. Comparison of the spectra illustrated in Fig.6 with EPR spectra of arenecyclopentadienyliron,[33] in which the iron atom has the $3d^7a_{1g}^2e_{2g}^4.e^{*1}_{1g}$ configuration (d_{xz} and d_{yz} are the orbitals of the unpaired electron) demonstrates the similarity of the *g*-factors and of the degrees of their anisotropy. It may be that the presence of the cyclopentadienyl ligand in these two different complexes is responsible also for the analogous disposition of the *d* levels[33].

More complex reactions are observed for the molybdenum and tungsten complexes. The primary ligand-centered radicals are converted into metal-centered radicals of two types: the first has the structure (XVIII) and the second has the structure (XIX) (see Table 3):[43]



The radicals of type (XVIII) are unstable and are converted into the radicals (XIX) in the presence of an *o*-quinone. Complexes of type (XVIII) are characterised by $g < 2$, but the deviations from 2 are not as great as in complexes of type (XIX); the *g*-factor for the complex (XVIII) (M = Mo) is almost isotropic. The spectrum of this radical is characterised[43] by an HFC constant of 15.6 G corresponding to coupling with the ^{95}Mo(^{97}Mo)nuclei ($I = 5/2$) and with two protons of the catechol ligand. We may note the small (~1 G) splitting by the protons compared with the splitting of 3.5 G characteristic of the corresponding *o*-semiquinolates.

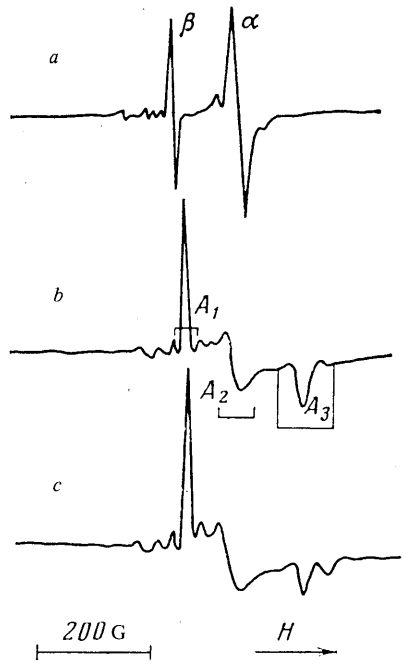


Figure 6. EPR spectra of tungsten complexes: *a*) $(3,6\text{-Q})_2.\dot{W}C_5H_5$ (α, the satellite lines due to ^{183}W are visible) at −20 °C (*1*) and $(3,6\text{-Q})_2\dot{M}oC_5H_5$ (β) present in solution as a consequence of a slight admixture of $Mo_2(C_5H_5)_2(CO)_6$ in the initial dimer $W_2(C_2H_5)_2(CO)_6$; *b*) $(3,6\text{-Q})_2\dot{W}C_5H_5$, −155 °C ($A_1$, A_2, and A_3 are the components of the tensor of the hyperfine coupling with the ^{183}W nuclei); *c*) mixture of $(3,6\text{-Q})_2WC_5H_5$ (*1*) and $3,6\text{-QCl}_4\text{Q}WC_5H_5$ (*2*), −155 °C.[43]

It is so far difficult to put forward a mechanism for the transfer of spin density from the metal atom and to estimate its value in the *o*-quinone ligand. One can only claim that in the secondary molybdenum complex there is one *o*-quinone ligand symmetrically attached to the molybdenum atom. The substitution of the remaining two CO groups in the radical (XVIII) (M = Mo) by the *o*-quinone ligand decreases the average *g*-factor and leads to the appearance of a considerable anisotropy of the latter (see Fig.5 and Table 3) and to an increase of the constant for hyperfine coupling with the ^{95}Mo(^{97}Mo)nuclei.[43]

The factors g_2 and g_3 proved to be sensitive to the structure of *o*-quinone following the replacement of 3,6-Q and 3,5-Q by Cl_4Q^-. The presence of two molecules of the *o*-quinone ligand in the complex (XIX) has been confirmed by the formation of mixed complexes. The interaction of $\dot{M}o(C_5H_5)(CO)_3$ with a mixture of 3,6-Q and *o*-chloranil produces, together with $(3,6\text{-Q})_2\dot{M}o(C_5H_5)$, also the complexes $(Cl_4Q)_2\dot{M}o(C_5H_5)$ and $(3,6\text{-Q})\,(Cl_4Q^-)\dot{M}o(C_5H_5)$.[43] The formation of $(3,6\text{-Q})\,(Cl_4Q)\dot{M}o(C_5H_5)$ was inferred from the appearance of a new line characterised by a value of g_3 different from that for the individual complexes of 3,6-Q and Cl_4Q. The relative intensities of the signals of the individual and mixed complexes depend on the ratio of the *o*-quinones 3,6-Q and Cl_4Q. The value of g_3 for the mixed complex is approximately equal to its average value for the individual complexes[43].

An analogous behaviour has been observed in the study of tungsten-containing complexes. The metal-centered radical (XVIII) is less stable and does not accumulate at high concentrations, being rapidly converted into the radical (XIX). The spectra of the tungsten complexes (XIX) exhibit larger shifts of the *g*-factor and a higher degree of anisotropy of the latter compared with the molybdenum complexes, possibly as a consequence of the larger spin-orbital coupling constant[34]. The interaction with a mixture of 3,6-Q and Cl_4Q results in the formation of mixed complexes characterised by smaller values of g_3 than for the 3,6-Q complex; the individual complex (XIX) with Cl_4Q is not formed. The parameters of the spin-Hamiltonian for the molybdenum complex (XIX) are close to the analogous parameters of the inorganic oxo-complexes described in the literature[35]. In the complexes $MoOX_4Y$ the molybdenum atom is located in the same plane as the ligands X_4; the complex has the C_{4v} symmetry, which is reflected by the axial symmetry of the *g*-factor, persisting even in mixed complexes of the type $MoOX_{4-i}Y_{i+1}$.[35] Presumably the absence of axial symmetry in the complexes investigated is associated, on the one hand, with the presence of the cyclopentadienyl ligand and, on the other hand, with the absence of the C_{4v} symmetry in the disposition of the oxygen atom relative to the $Mo-C_5H_5$ bond.

The electronic structure $4d^1$, with localisation of the unpaired electron in the d_{xy} orbital lying in the plane of the ligand X_4, is characteristic of the oxomolybdenum(V) complexes. The parameters of the spin-Hamiltonian of the oxo-complexes are extremely sensitive to the substitution of the ligand X_4.[35] In the oxo-complexes of *o*-quinones there is a catecholate linkage with the molybdenum(VI) atom[36]. All these factors suggest that the electronic configuration $4d^1$, with localisation of the unpaired electron in the d_{xy} orbital, is characteristic of the complex $Q_2\dot{M}oC_2H_5$. An analogous hypothesis can apparently be put forward also for the tungsten complex in view of the similarity of the EPR spectra.

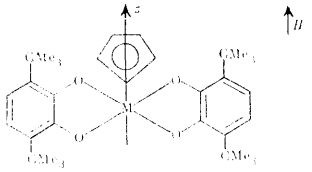
This hypothesis is confirmed by the analysis of the anisotropy of the *g*-factor and the anisotropic component of the HFC constant for the molybdenum and tungsten complexes. Having adopted the $4d^1$ state of the unpaired electron (the d_{xy} orbital) as the ground state and having neglected the delocalisation of the unpaired electron density over the ligand, we obtain the following expressions:

$$g_z = 2 - \frac{8\xi_M}{E_{d_{x^2-y^2}} - E_{d_{xy}}};\quad g_x = 2 - \frac{2\xi_M}{E_{d_{xz}} - E_{d_{xy}}};\quad g_y = 2 - \frac{2\xi_M}{E_{d_{yz}} - E_{d_{xy}}}\ .$$

Hence it follows that most probably $g_z = g_3$.

It follows from Figs.5 and 6 that there is no axial symmetry of the anisotropic hyperfine coupling either. The values $A_1 = 41$ G, $A_2 = 60$ G, and $A_3 = 112.5$ G for the tungsten complex (XIX) ($I^{183}W = 1/2$) can be determined from the EPR spectrum of a frozen solution, illustrated in Fig.6*b*. The value $\bar{A} = (A_1 + A_2 + A_3)/3 = 71.2$ G is close to $A_{iso} = 72.5$ G determined from the spectrum of the solution (Fig.6*a*). The values $A_1 = 66.0$ G and $A_3 = 65.0$ G for the complex $(3,6\text{-Q})_2MoC_5H_5$ can be determined from the spectrum; $A_2 = 113.0$ G has been calculated from the relation $A_{iso} = (A_1 + A_2 + A_3)/3$.

The dipole–dipole components of the HFC constant (A^P) can be determined from these data. For the molybdenum complex, we have $A_1^P = -2.0$ G, $A_2^P = 25.0$ G, and $A_3^P = 27.0$ G, while for the tungsten complexes the corresponding values are -31.5, -12.5, and 40.0 G. The identical signs of A_3^P and A_{iso}^P are consistent with the fact that the unpaired electron occupies the d_{xy} orbitals and the values of g_3 and A_3 correspond to the orientation of the *z* axis parallel to the external magnetic field[36].

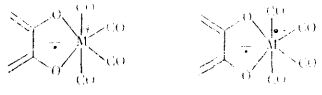


On the basis of the above considerations concerning the electronic structure of the molybdenum and tungsten complexes of type (XIX), one can postulate that complexes of type (XVIII) should also have the $4d^3$ and $5d^3$ configurations.

Transition metal complexes with *o*-quinone ligands can be obtained by the photochemical reaction of *o*-quinones with metal carbonyls. The photolysis of $Mo(CO)_6$ in the presence of 3,5-di-t-butyl-*o*-quinone, *o*-chloranil, and phenanthrenequinone yields complexes of different compositions[4,14]. The compositions were established by X-ray diffraction and were found to be represented by the formulae $\{MoO[O_2C_6H_2\cdot(t\text{-}Bu)_2]_2\}_2$ for 3,5-di-t-butyl-*o*-quinone,[36] $Mo(O_2C_6Cl_4)_3]_2$ for *o*-chloranil,[37] and $(PhenQ)_2Mo_2O_5(PhenQ)_2$ for phenanthrenequinone.[38]

There is at present not only no clear-cut idea about the mechanism of these reactions and about the dependence of the final products on the nature of the *o*-quinone but even the source of the oxygen atoms of the oxomolybdenum group is not known exactly. Although $MoO[O_2C_6H_2(t\text{-}Bu)_2]_2$ was synthesised in an N_2 atmosphere, the possible role of the presence of traces of oxygen in the formation of the main reaction product has been assumed[36]. The application of the EPR method to the study of the reaction mechanism did not yield an umambiguous answer to the question of the structure of the paramagnetic species detected and of their role in the formation of the final diamagnetic products[4,28].

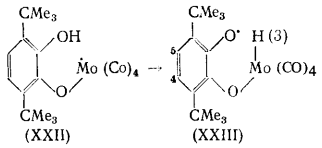
On the basis of the analysis of the EPR spectra of the semiquinone species arising in the photolysis of tungsten and molybdenum hexacarbonyls in the presence of phenanthrenequinone, formula (XX) was attributed to these species.



(XX) (XXI)

Here the metal is in the +1 oxidation state[28]. Since the unpaired electron of the ligand in compounds of type (XX) arises as a result of electron transfer from a metal atom having an odd number of electrons, in reality the metal atom should also carry an unpaired electron and the system as a whole should have a biradical character; formula (XXI) corresponds to this situation.

The reaction between $Mo(CO)_6$ and 3,6-di-t-butyl-*o*-quinone (3,6-Q) in pentane under vacuum conditions on irradiation with the light of a mercury lamp at room temperature is accompanied, as in the study of Weir and Wan[28], by the formation of the *o*-quinone radical-anions without any signs of hyperfine coupling with the molybdenum isotopes. Weir and Wan[28] present some arguments in support of the assignment of the measured spectra to a complex of type (XX) but, in view of the absence of hyperfine coupling with the magnetic molybdenum isotopes, this assignment cannot be regarded as unambiguous. When the above reaction is carried out at low temperatures, species whose EPR spectra are characterised by the following HFC constants are formed: $a_{H(3)}$ = 0.16 G, $a_{H(4)}$ = 3.8 G, $a_{H(5)}$ = 3.0 G, and a_{Mo} = 1.9 G.[54] The low constants for hyperfine coupling with one of the protons in the ^{95}Mo and ^{97}Mo isotopes enabled Sarbasov et al.[54] to propose the oxygen-centered structure (XXIII) for the species formed. The small difference between the constants for the hyperfine coupling with the protons in the fourth and fifth-positions of the aromatic ring shows that the bond between the central molybdenum atom and oxygen is polar under these conditions:

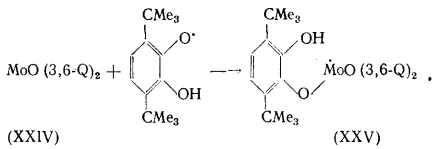


The formation of the radical (XXIII) should apparently be preceded by the formation of the metal-centered radical (XXII). The formation of these radicals is probably associated with the involvement of the semiquinone radical, functioning as a monodentate ligand. The participation of the semiquinone radical in the reaction is indicated by the increase of the concentration of the radicals (XXIII) when hydroquinone is added to the system.

Thus the reaction of the photoexcited quinone with hydrogen atom donors must be added to the primary photochemical step in the formation of the complexes, consisting in the elimination of the CO group from $Mo(CO)_6$.[28,29] After prolonged photolysis (~30 min) at a low temperature, a paramagnetic complex, in which the unpaired electron is localised at the molybdenum atom, accumulates gradually together with the unstable radical (XXIII).[54] When the reaction is carried out at room temperature, the radical (XXIII) is not formed at a concentration sufficiently high for measurement, but an increase of temperature does not affect the formation of the molybdenum-centered free radical. This radical is stable at room temperature *in vacuo* but disappears when oxygen is admitted into the tube.

The identification of the paramagnetic complex described as a molybdenum-centered free radical is based on the following spectroscopic data: the appreciable difference of the *g*-factor from 2, the appreciable anisotropy of the *g*-factor, and the large constants for splitting by the Mo nuclei[54].

According to the results of chemical analysis[36], one can postulate the formation of mainly the diamagnetic product $MoO[O_2C_6H_2(t\text{-}Bu)_2]_2$. The presence of the M=O bond in the photolysis product follows from the formation of the paramagnetic complex when the reaction mixture is treated with HCl,[54] because the *g*-factor and the HFC constant for the complex formed are fully consistent with the known values for $MoOCl_5$.[35] The similarity of the spectral parameters of the radicals listed in Table 4 is striking. On this basis, one can suggest that these spectra correspond to radicals arising via the reaction[54]



The interaction of (XXIV) and (XXV) with HCl leads to the formation of $MoOCl_5$.

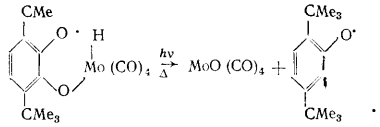
It follows from Table 4 that the parameters of the EPR spectra depend on the solvent and on the structure of the *o*-quinone. The influence of THF is evidently associated with complex formation.

Table 4. The *g*-factors and the constants for the hyperfine coupling with the molybdenum nucleus in the hydroxy-molybdenum complexes of *o*-quinones[54].

Complex	a_{Mo}, G	$\bar{g}$	g_1	g_2	g_3
(XXV) in THF*	46.5	1.953	1.985	1.945	1.945
(XXV) in pentane	51.9	1.939	1.961	1.940	1.917
$MoOCl_5$ in THF	51.9	1.946	1.968	1.942	1.942

*Axial symmetry.

It follows from the analysis of the X-ray diffraction data that the *o*-quinone ligand in $(MoOQ_2)_2$ [36] accepts two electrons from the metal atom and is a catecholate dianion. The source of the oxygen atoms in the oxomolybdenum group remains unelucidated. The formation of the M–O bond *in vacuo* suggests that the source of the oxygen atoms is some kind of complex of the *o*-quinone whose cleavage gives rise to the M=O bond, for example:



The photolysis of $Mo(CO)_6$ in toluene in the presence of di-t-butyl peroxide also leads to the appearance of a signal with a slightly anisotropic *g*-factor (g = 1.931), tentatively identified as $t\text{-}BuOMo(CO)_4$.

3. The Electronic Structure of the Tris-3,6-di-t-butyl-*o*-quinone Complexes of Chromium

Numerous studies have now been devoted to the tris-*o*-quinone complexes of chromium[4,39]. They are believed to be the closest analogues of the bacterial iron complex of the siderphore enterobactin[40]. There is so far no unanimous view concerning the electronic structure of these complexes. On the basis of the analysis of the X-ray diffraction data for the tris-3,5-di-t-butyl-*o*-quinone complex of chromium, Downs et al.[41] concluded that the Cr^{3+} ion is coordinated to three semiquinone ligands. After analysing the same data, Sofen et al.[39] concluded that the Cr^{3+} ion is coordinated to non-reduced *o*-quinone molecules. The difference between the studies of Downs et al.[41] and Sofen et al.[39] is associated with the fact that the former authors estimated the degree of reduction of the ligand from the length of the C–O bond,

while the latter estimated it from the length of the C–C bonds in the ring. According to polarographic data, the complexes should reversibly accept and give up six electrons[39,41]. The electronic absorption spectra of the tris-3,5-di-t-butyl-o-quinone complex of chromium and of its mono-, di-, and tri-anions in the visible region have been recorded[39].

The EPR spectra of the radical-cations and radical-anions exhibit a surprising similarity, which is manifested in the similarity of the constants for hyperfine coupling with the ^{53}Cr nuclei and of the g-factors.[55] The appreciable deviation of the g-factor from 2.0023 and the large splitting by ^{53}Cr (20–30 G) show that an appreciable fraction of the unpaired electron in the radical-cations and radical-anions is localised at the chromium atom[4,41]. It has been suggested that, on passing from the radical-cation to the radical-anion, the levels of the metal and ligands are inverted, so that in both cases the d_{z^2} orbital of the chromium atom accommodates the unpaired electron[4].

Until recently, there were no data on the distribution of the unpaired electron density among the o-quinone ligands, without which the description of the distribution of the spin density is incomplete. Such data have been obtained in a study[55] of the EPR spectra of the radical-cations and radical-anions of the tris-3,6-di-t-butyl-o-quinone complexes of chromium. The corresponding radical-cation and radical-anion were obtained by oxidising the tris-3,6-di-t-butyl-o-quinone complex of chromium with I_2 and by reducing it with the sodium and potassium salts of n-Bu_4NOH in solution in THF. The radical-cation is reformed on treating the radical-anion with I_2. The reversibility of the reduction has been established by the EPR method and electronic absorption spectroscopy. Figs.7 and 8 present the EPR spectra of the radical-cations and radical-anions of the complexes. The EPR spectrum of the radical-cation is characterised by the following parameters: g = 1.9689, a_{Cr} = 25.5 G, and a_H = 0.85 G.

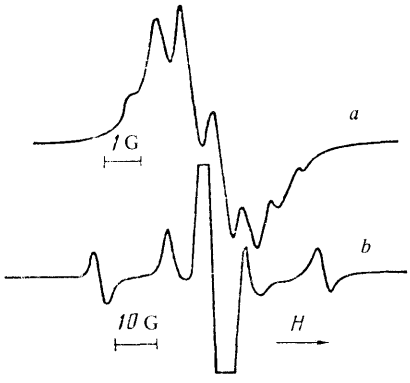


Figure 7. EPR spectrum of the radical-cation $Cr(3,6\text{-}Q)_3^+I^-$ in THF; spectrum *b* was recorded with tenfold amplification relative to spectrum *a*.[55]

For the semiquinone type of distribution of spin density in the ligand, there is a splitting of 0.85 G which corresponds to a spin density of 0.7 in the three o-quinone ligands, since the corresponding splitting in the radical-anion of 3,6-di-t-butyl-o-quinone is 3.6 G. This implies that the maximum spin density, amounting to 0.3, corresponds to the chromium atom, while in an individual ligand it amounts to 0.23.

The EPR spectrum of the radical-anion is characterised by the following parameters: g = 1.9707, a_{Cr} = 22.7 G, and a_H = 0.85 G.[55] The main difference between the spectrum of the radical-anion and that of the radical-cation consists in a decrease of the hyperfine coupling with ^{53}Cr and an appreciable increase of the line width. The best resolution is observed in the temperature range from 0° to –20 °C. At these temperatures, one of the wings of the envelope curve in Fig.8 shows clearly three HFS components. Presumably the number of lines is not less than seven, i.e. the unpaired electron density is delocalised over three ligands in the radical-anion, as in the radical-cation. It has been observed that the HFS pattern is independent of the nature of the cation (sodium or potassium).

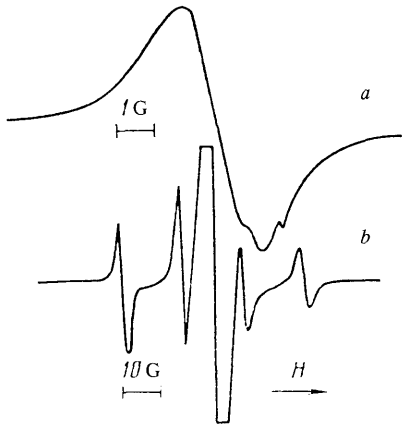
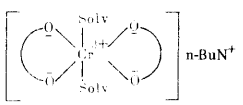


Figure 8. EPR spectrum of the radical-anion $Cr(3,6\text{-}Q)_3^-Na^+$ in THF; spectrum *b* was recorded with twentyfold amplification relative to spectrum *a*.[55]

Thus it follows from the data obtained that the distribution of spin density in the radical-anion is the same as in the radical-cation. Previously it had been assumed that in the paramagnetic chromium complexes the bulk of the unpaired electron density is located at the chromium atom[4]. We can now claim that the bulk of the spin density is in fact located in the ligands and not at the chromium atom.

The EPR spectra of the di-o-quinone complexes of chromium in the radical-cationic and radical-anionic forms have also been obtained[55]. These complexes are formed on prolonged treatment of the electrically neutral complex with oxidants and reductants and also as a result of the photochemical reactions of 3,6-di-t-butyl-o-quinone with $Cr(CO)_6$. In contrast to the tris-o-quinone complexes, the character of the distribution of spin density in the radical-cations and radical-anions of the di-o-quinone complexes of chromium is completely different. Five HFS components with a binomial distribution of intensities and the splittings a_H = 0.85 G and $a_{^{53}Cr}$ = 25.5 G are clearly seen in the EPR spectrum of the radical-cation obtained by the prolonged treatment of $Cr(3,6\text{-}Q)_3$ with I_2. It follows from these data that the spin densities are 0.46 in the two ligands and 0.54 at the chromium atom[55].

After the reduction of $Cr(3,6\text{-}Q)_3$ with n-butyl alcohol, the EPR spectrum of the reaction mixture shows, apart from the signals due to the chromium atoms, $(3,6\text{-}Q)_3^{\bullet}$, and $(3,6\text{-}Q)^{\bullet-}$, a narrow signal with chromium satellites (a_{Cr} = 16.0 G).[55] The narrow signal is apparently due to the radical-anion $Cr(3,6\text{-}Q)_2^{\bullet}$, which is formed after the elimination of $(3,6\text{-}Q)^{\bullet-}$ from the initial radical-anion. The absence of hyperfine coupling with the ligand protons indicates the localisation of the unpaired electron at the chromium atom, which led to the assignment of the biscatecholate structure (XXVI) to these species:



(XXVI)

Analysis of the parameters a_{Cr} for the test complexes shows that they are influenced by the spin densities both at the chromium atom and at the oxygen atoms. The radical-cations described above are obtained on photolysis of 3,6-Q and $Cr(CO)_6$. In this case they are formed either under the influence of traces of O_2 or on irradiation[55].

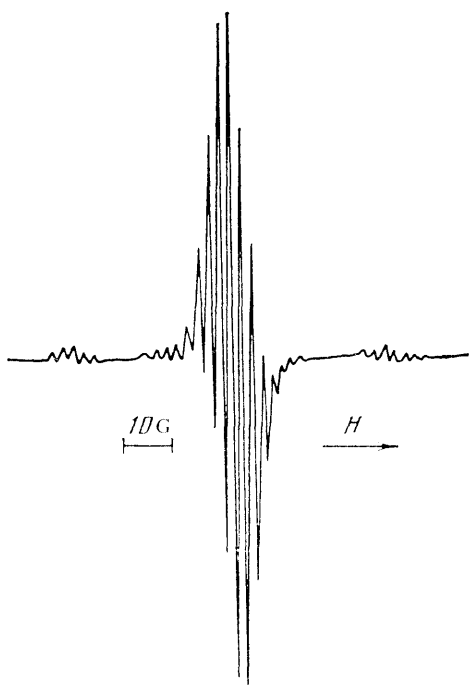


Figure 9. EPR spectrum of the radical cation $Cr(CF_3\text{–}\overset{O}{\overset{\|}{C}}\text{–}\overset{O}{\overset{\|}{C}}\text{–}CF_2CF_3)_2^{+\bullet}$.[42]

In addition to the tris-3,6-Q complexes of chromium, the di-*o*-quinone complexes of chromium are also formed in coordinating solvents (ether, THF, and alcohol). It is noteworthy that, after the photolysis of a solution of 3,5-Q and $Cr(CO)_6$ in toluene, the EPR spectrum exhibits a HFS corresponding to the three protons of the three *o*-quinone ligands; the splittings are $a_H \cong 1.00$ G and a_{cr} = 26.9 G, while g = 1.9731.[55]

Fig. 9 presents the EPR spectrum obtained on photolysis of $CF_3\text{–}\overset{O}{\overset{\|}{C}}\text{–}\overset{O}{\overset{\|}{C}}\text{–}CF_2\text{–}CF_3$ in an α-diketone in the presence of $Cr(CO)_6$. Analysis of the HFS shows that there are two α-diketone ligands in the radical-cation complex (a_F = 2.8 G, a_{cr} = 27 G, and g = 1.9658). The parameter a_F = 8.8 G has been obtained for the corresponding semidione complex of $Mn(CO)_4$, where the unpaired electron is localised in the ligand[42]. It follows from a comparison of these data that 0.6 of the unpaired electron density in the radical-cation complex of chromium corresponds to the two ligands and 0.4 corresponds to the chromium atom. Presumably two coordination sites in the two-ligand complexes are occupied either by CO groups or solvent molecules.

Whereas the distribution of the spin density of the unpaired electron can be inferred from EPR data, the distribution of the charge can be postulated solely on the basis of indirect data. For the purpose of further study of the electronic structure of the complexes, their electronic absorption spectra were obtained. Previously Solodovnikov et al.[20] investigated the influence of coordination on the positions of the absorption bands of the semiquinone chromophore in relation to the carbonylmanganese and carbonylrhenium complexes of 3,6-Q. Comparison of the spectrum of $Cr(3,6\text{-}Q)_3$ with that of $Cr(3,5\text{-}Q)_3$ [39] showed the complete identity of the positions and intensities of the absorption bands in the visible regions: in the ultraviolet region[55], a band was recorded at 290 nm (Fig. 10). Comparison of the positions and intensities of the absorption bands in the $Cr(3,6\text{-}Q)_3$ spectrum with the positions and intensities of the absorption bands in the spectra of $(3,6\text{-}Q)^{\bullet-}Na^+$ and $(3,6\text{-}Q)^{\bullet-}\,Mn^+(CO)_4$ [20] as well as other manganese and rhenium complexes leads to the conclusion that the electronic configuration of the complex is much closer to that of $Cr^{3+}(3,6\text{-}Q)_3^{\bullet}$ than to the configuration of the complex $Cr(3,6\text{-}Q)_3$.[55]

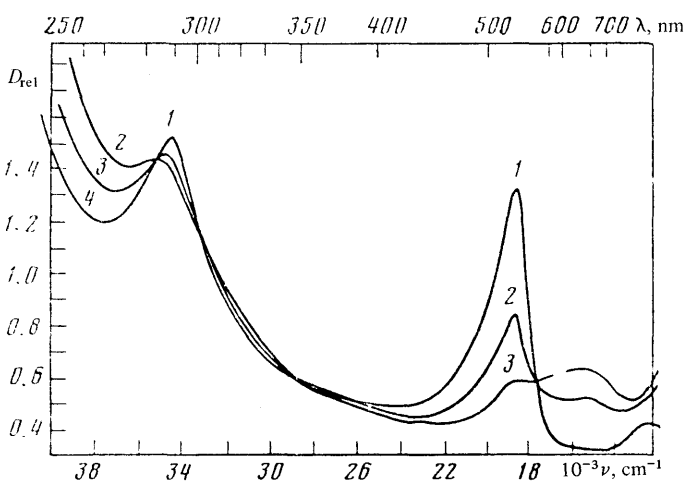


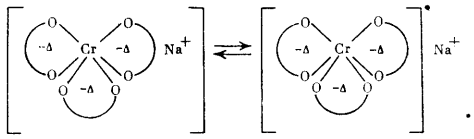
Figure 10. The changes in the electronic absorption spectra of $Cr(3,6\text{-}Q)_3$ during reduction by n-Bu_4NOH in THF: *1*) $Cr(3,6\text{-}Q)_3$; *2*) spectrum corresponding to the intermediate reduction stage; *3*) $Cr(3,6\text{-}Q)_3^{\bullet-}n\text{-}Bu_4N^+$.[55]

The reduction of the complexes *in vacuo* on a sodium mirror leads to a sharp decrease of the intensity of the 525 nm band and to the appearance of new absorption bands

at 520, 575, and 680 nm and a band with $\lambda_{max} > 800$ nm, which can probably be identified, on the basis of the study of Sofen et al.[39], as the 825 nm band. Measurement of the spectra in the course of the reduction of the complex revealed an isosbestic point; the spectrum *3* has been assigned to $Cr(3,6\text{-}Q)_3^{-}$.[55]

The large number of absorption bands in the spectrum of $Cr(3,6\text{-}Q)_3^{-}$ is striking. In view of this and also in view of the behaviour of the line width in the EPR spectrum of the complex $Cr(3,6\text{-}Q)_3^{-}Na^+$, the problem arises as to the form of the distribution of negative charge and spin density and of the influence of the cation on this distribution. In order to solve this problem, the complex was reduced by n-Bu_4NOH (Fig.10). The spectrum of $Cr(3,6\text{-}Q)_3^{-}n\text{-}Bu_4N^+$ differs from that of $Cr(3,6\text{-}Q)_3^{-}Na^+$ by the absence of the band at 575 nm.

The study of the influence of temperature on the spectrum of $Cr(3,6\text{-}Q)_3^{-}Na^+$ showed that the intensity of the 575 nm band diminishes appreciably when the temperature is reduced from 50° to −70 °C. This entails some increase of the intensity of the 680 nm band. Presumably the 575 nm absorption band is associated with the formation of a contact pair:



The temperature dependence of the width of the EPR line of the radical-anion may be partly associated both with the presence of this equilibrium and with the migration of Na^+ between the ligands in the contact and solvent-separated ion pairs. The use of n-Bu_4N^+ as the cation does not entail line narrowing. The subsequent reduction of $Cr(3,6\text{-}Q)_3^{-}Na^+$ on a sodium mirror leads to the disappearance of the 575 and 825 nm bands. The spectrum of $Cr(3,6\text{-}Q)_3^{2-}.2Na^+$ in the visible region consists of two bands at 516 and 720 nm. On reduction with atmospheric oxygen, the spectrum of the dianion gradually disappears and that of the radical-anion reappears; the radical-anion is stable in air for a long time.

The oxidation of the complex by oxidants such as I_2 and $AgBF_4$ is accompanied by a decrease of the intensity of the 525 nm band and the appearance of a new band at 365 nm in the electronic absorption spectra.

The experimental data presented yield a qualitative picture of the electronic structure of $Cr(3,6\text{-}Q)_3$ and its oxidised and reduced forms. We established that the degree of reduction of the ligand in $Cr(3,6\text{-}Q)_3$ is close to that in the semiquinone, while in the radical-cation and the radical-anion most of the spin density (0.7) is located in the ligands. On this basis, one can postulate that the number of electrons in the ligands of the radical-cation should be close to an odd number, for example 2.7; the number 1.7 no longer satisfies this condition. When the negative charge in the ligand is −2.7e, the charge on the chromium atom should be +3.7e. The number of electrons in the ligand of the radical-anion should be 4.7 and the charge on the cation should be +3.7e. Presumably in the electrically neutral complex the same charge of +3.7e on the chromium atom remains and the overall charge of the ligands is −3.7e. According to this picture, the charge on the chromium ion (+3.7e) in the complex does not change on oxidation and reduction.

According to the proposed charge distribution in the ion pairs involving the radical-cations and radical-anions, a completely different interaction between the counterions should be observed: in the former case there should be a weak interaction owing to the shielding of the positive charge on the chromium atom by the negatively charged ligands and in the latter case there should be a strong interaction due to the high negative charge on the ligands. The differences between the widths of the EPR lines of the radical-cations and radical-anions, caused by the difference in the dynamics of the redistribution of the spin and charge densities between the ligands and the complex, may be associated with this factor.

In conclusion it is useful to compare the spin density on the chromium atom, which amounts to 0.3, with the spin density in the ligand (0.23). The localisation of the unpaired electron either in the ligand (Mn, Re) [22,23] or at the central metal atom (W, Mo) [43] is characteristic of the majority of the transition metal complexes with semiquinone or catechol ligands investigated hitherto. The similarity of the spin densities on the chromium atom and in one of the ligands indicated above demonstrates the approximately equal involvement of their orbitals in the formation of a bond. Thus one may conclude that the Cr=O bond is highly covalent. It may be that the high degree of covalence of the M−O bond is the cause of the high complex forming capacity of enterobactin towards Fe^{3+} and Cr^{3+}.

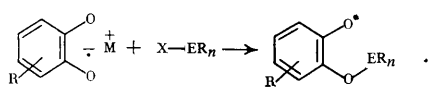
III. THE STEREOCHEMISTRY OF PARAMAGNETIC CHELATE COMPLEXES OF GROUP IV ELEMENTS WITH SEMIQUINONE LIGANDS

Within the framework of the electronic structures (I)−(V), the degree of reduction of the *o*-quinone ligand in the paramagnetic complexes of Group IV elements is −1. The main task of the study is to determine the coordination of the semiquinone ligand and the structure of the complex. Depending on the same variables (M, X, and *n*), not only are different types of coordination observed [structures (III) and (IV)] but also there is a significant variation in the geometrical disposition of the ligands X relative to the central atom M. Whereas the octahedral structure is characteristic of transition metal complexes of *o*-quinones, for the complexes of Group IV elements considerable variety of different types of environment of the central atom is observed. Analysis of the hyperfine coupling of the unpaired electron of the *o*-semiquinone ligand with the magnetic moments of the nuclei of the elements incorporated in the ligand X makes it possible to infer the geometrical disposition of these elements.

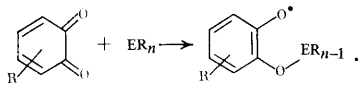
The different dispositions of the ligands relative to the plane (the nodal plane for the π orbitals of the unpaired electron localised in the *o*-semiquinone ligand) formed by the atom M and two oxygen atom is manifested by the equal values of the HFC constants. The non-equivalence of the oxygen atoms in the chelate coordination of the *o*-semiquinone ligand can arise in its turn in structures characterised by a trigonal-bipyramidal geometry of the disposition of the ligands X around the atoms M. This non-equivalence should be manifested by the inequality of the constants for the hyperfine coupling of the unpaired electron with different ring protons of the ligand [for example, $a_{H(4)} \neq a_{H(5)}$ in the case of the 3,6-di-t-butyl-1,2-dihydroxybenzene ligand].

Chelate *o*-semiquinone complexes of Group (IV) elements can be obtained from the following reactions.

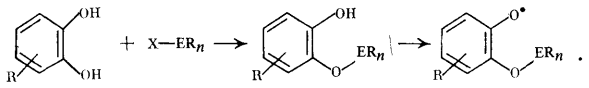
1. The interaction of alkali metal *o*-semiquinolates with organometallic halogeno-derivatives:



2. The interaction of *o*-quinones with organometallic compounds:

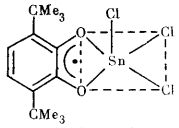


3. The interaction of catechols with halogeno-derivatives and subsequent oxidation of the hindered phenols formed:



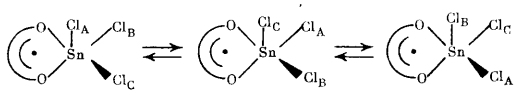
1. Pentacoordinate Chelate Complexes

The *o*-benzosemiquinone complex (XXVII) has been obtained by the reaction of tin tetrachloride with 3,6-di-t-butyl-*o*-benzoquinone (3,6-Q) [44] in toluene. Hyperfine coupling with two equivalent protons [$a_{H(4)} = a_{H(5)} = 3.9$ G], one $^{35,37}Cl$ nucleus ($I = 3/2$, $a_{Cl} = 0.6$ G), and the magnetic isotopes ^{117}Sn and ^{119}Sn ($a_{^{117}Sn} = a_{^{119}Sn} = 7.2$ G) has been recorded for this compound at room temperature. The spectroscopic data obtained led to the conclusion that the complex (XXVII) formed has a chelate tetragonal-pyramidal structure (see Fig.11*a*):[44]



(XXVII)

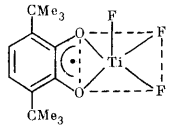
This structure explains why hyperfine coupling with only one chlorine nucleus was recorded: the other two lie near the nodal plane of the π orbital of the unpaired electron and hyperfine coupling with them is not manifested in the spectrum. With increase of temperature in the range 40–80 °C, the HFS lines are broadened due to the coupling with the chlorine nucleus and above 100 °C each component of the proton triplet is split into ten lines (Fig.11*b*) due to the hyperfine coupling with the three equivalent chlorine atoms ($a_{Cl} = 0.3$ G). The temperature-induced changes are fully reversible and indicate the presence of a dynamic effect due to the rotation of the $SnCl_3$ group relative to the plane of the *o*-semiquinone ligand at an elevated temperature. This rotation can be considered from the standpoint of the "tourniquet" mechanism proposed for compounds with a pentacoordinate phosphorus atom[45,46]:



As a result of such rotation, all three chlorine nuclei become equivalent and the constant for hyperfine coupling with the $^{35}Cl(^{37}Cl)$nuclei diminishes by a factor of 2 which is typical for hyperfine coupling with the β-nuclei in free radicals when the unpaired electron is delocalised via a hyperconjugation mechanism. The frequency of rotation in the range 20–50 °C has been estimated and is described by the expression[44]

$$\nu_{wt}(s^{-1}) = 2.4 \cdot 10^{15} \exp[-(13000 \pm 1000)/RT]; \nu_{rot}(20^\circ C) = 6 \cdot 10^5 s^{-1}.$$

The complex (XXVIII), obtained by the interaction of titanium tetrafluoride with 3,6-Q in toluene, has an analogous tetragonal-pyramidal structure[56]. Triplet splitting by two equivalent protons [$a_{H(4)} = a_{H(5)} = 3.8$ G], a doublet due to the ^{19}F nucleus, located outside the nodal plane ($a_{^{19}F} = 4.7$ G), and a narrow triplet due to two fluorine nuclei, located in the vicinity of the nodal plane ($a_F = 0.6$ G) (Fig.12) are recorded in this case.



(XXVIII)

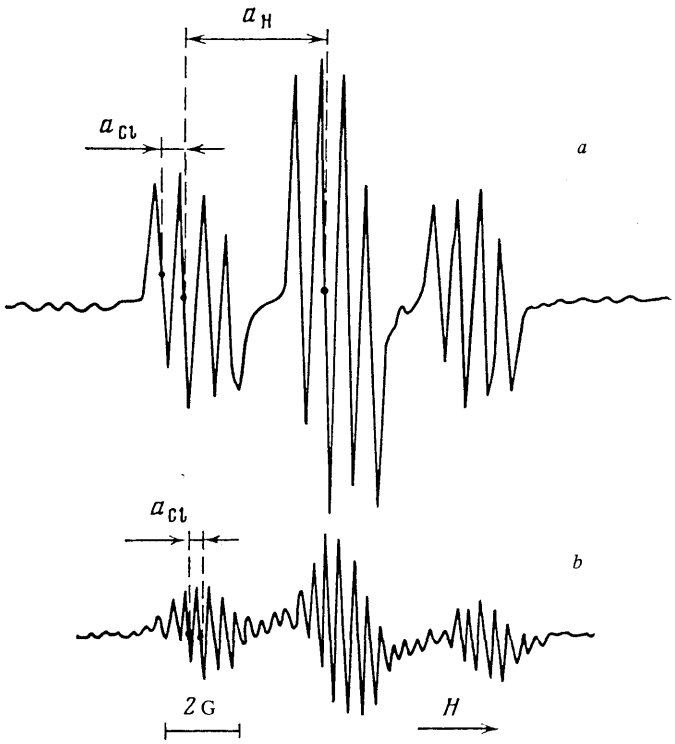


Figure 11. EPR spectrum of the complex (XXVII) in solution in toluene at 0 °C (*a*) and 100 °C (*b*).[44]

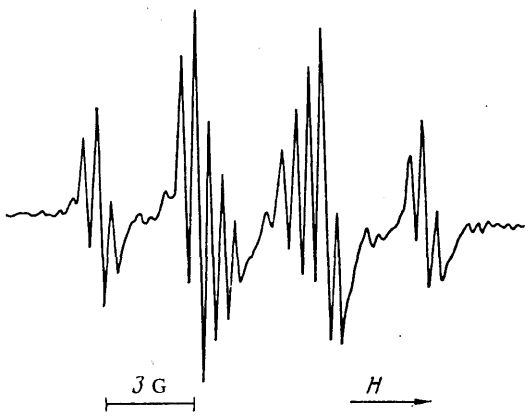


Figure 12. EPR spectrum of the complex (XXVIII) in toluene at 20 °C.[56]

The HFC constants (3.8 G) were assigned to two protons of the *o*-semiquinone ligand on the grounds that their sum [$a_{H(4)} + a_{H(5)} = 7.6$ G] is typical for organoelemental radicals with 3,6-di-t-butyl-1,2-dihydroxybenzene ligands. The greater magnetic moment of the ^{19}F nuclei compared with the $^{35}Cl(^{37}Cl)$ nuclei as well as the small size of the central atom compared with tin are responsible for the higher constants for the hyperfine coupling with these nuclei and also for the detection of the hyperfine coupling with the fluorine nuclei located in the vicinity of the nodal plane in this case. Over the entire temperature range (from -80° to 100 °C), the spectral pattern remains unchanged, which is apparently associated with the low frequencies of rotation of the TiF_3 groups relative to the plane of the catechol ligand[56].

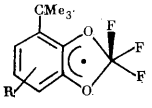
Hyperfine coupling with three nonequivalent nuclei having a spin of 1/2 (the HFC constants are 3.5, 4.2, and 4.9 G) and with the ^{117}Sn and ^{119}Sn nuclei has been recorded in toluene for the 3,6-di-t-butyl-*o*-semiquinone complex containing the SnF_3 group[55]. The HFC constants amounting to 3.5 and 4.2 G were assigned to the protons of the *o*-semiquinone ligand on the basis of their characteristic sum, which is 7.7 G.[47] Correspondingly, the HFC constant equal to 4.9 G was assigned to the ^{19}F nucleus located outside the nodal plane. Since two structures—a tetragonal pyramid and a trigonal bipyramid—are possible for the pentacoordinate tin compounds, the observed non-equivalence of the ring protons can be explained by the distortion of the former structure towards the latter structure with an apical equatorial disposition of the *o*-semiquinone ligand. On the other hand, the non-equivalence of the ring protons in the trigonal bipyramid reflects the non-equivalence of the apical and equatorial E–O bonds[48].

Table 5. The spectroscopic parameters (G) of the radicals (XXIX)–(XXXI) in toluene at 20 °C.[56]

Radical	$a_{H(4)}$	$a_{H(5)}$	a_F^a	a_F^e
(XXIX)	4.2	3.6	0.35 (2)	10.1 (1)
(XXX)	—	3.8	1.0 (2)	9.7 (1)
(XXXI)	—	3.8	—	9.9

Note: the number of fluorine atoms is indicated in brackets. $a_H = 0.4$ G for the hydrogen atoms of the t-butyl groups in the radical (XXX); a_F^a and a_F^e refer respectively to the apical and equatorial positions of the ligand.

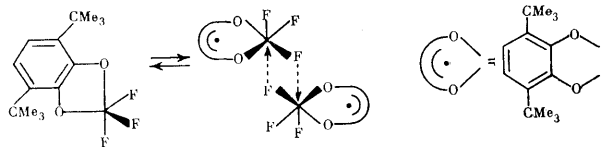
The structure of the trigonal bipyramid with an apical-equatorial disposition of the *o*-semiquinone ligand is characteristic of all the pentacoordinate silicon complexes which we investigated[49]. They were obtained by the reaction of SiF_4 with substituted *o*-quinones in weakly solvating media (toluene, ether). Table 5 presents the spectroscopic parameters for the complexes (XXIX), (XXX), and (XXXI) formed, on the basis of which it was concluded that they have a chelate trigonal-bipyramidal structure[56]:



(XXIX)–(XXXI)

where R = 6-t-butyl (XXIX), 5-t-butyl (XXX), or 5-trityl (XXXI). In this case the non-equivalence of the fluorine atoms is caused by their different steric dispositions relative to the nodal plane of the π orbitals of the unpaired electron. The non-equivalence of the ring protons of the 3,6-di-t-butyl-*o*-semiquinone ligand is caused by the non-equivalence of the apical and equatorial Si–O bonds in the trigonal bipyramid[49].

On reducing the temperature, spectroscopic changes were observed for the 3,6-di-t-butyl-*o*-semiquinone ligand, which can be explained by the association of the radical complexes (XXIX). This resulted in an alteration of the ratio of the constants for the hyperfine coupling with the ^{19}F nucleus and an additional hyperfine coupling (0.2 G), which we assumed to be due to the ^{19}F nucleus of another molecule of the complex, was recorded. The ring protons of the 3,6-di-t-butyl-*o*-semiquinone ligand then become equivalent:[50]



(XXIX)

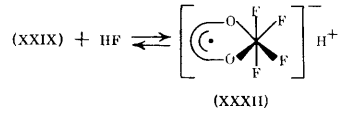
The spectra of the frozen solutions are characterised by an effective spin–spin interaction, which also confirms our hypothesis of the formation of associated species. On the basis of the zero splitting parameters obtained ($D = 316$ G, $E = 27$ G), the distance between the radical centres ($r = 4.4$ Å) was determined. The evolution of the spectra as a function of temperature is fully reversible.

Thus the coordination sphere of the central atom expands to six during the association process and there is a corresponding transition from the trigonal bipyramid to an octahedron, which is manifested spectroscopically by the appearance of a symmetrical distribution of the spin density (equivalent ring protons of the 3,6-di-t-butyl-*o*-semiquinone ligand) and the detection of hyperfine coupling with four fluorine nuclei.

Pentacoordinate tetragonal-pyramidal and trigonal-bipyramidal complexes of silicon, titanium, and tin exhibit electron-deficient properties and can coordinate additionally various electron-donating species (anions, solvent molecules) with formation of hexacoordinate octahedral radical-anions or molecular complexes.

2. Octahedral Chelate Complexes

In toluene which has not been carefully freed of moisture, the evolution of the spectra of the radical (XXIX) as a function of temperature differed significantly from that in dry toluene and corresponded to equilibrium between the radical (XXIX) and the radical-anion (XXXII) having an octahedral structure (Fig.13):[48]



(XXXII)

The change in the geometry of the complex from a trigonal bipyramid to an octahedron leads to the equalisation of the constants for the hyperfine coupling with the ring protons and the constants for the hyperfine coupling with the four ^{19}F nuclei, which are equal in pairs, are determined by their disposition relative to the nodal plane of the free-radical ligand. The evolution of the spectra as a function of temperature is fully reversible. The addition of diphenylamine or triethylamine to the reaction mixture fully displaces the equilibrium towards the radical-anion and the spectrum of

(XXXII) is recorded over the entire temperature range (up to 80 °C). Evidently the radical-anion complex is stabilised by the formation of an ammonium cation.

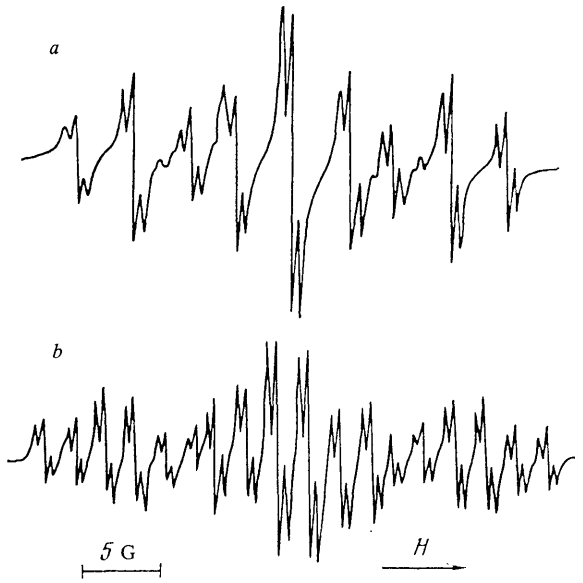
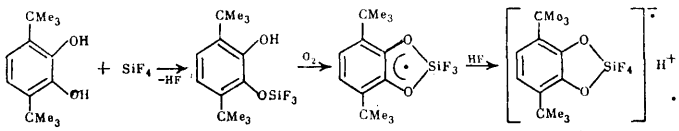
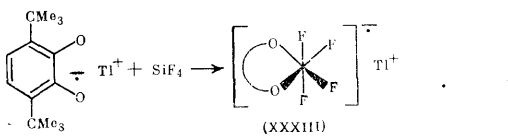


Figure 13. EPR spectra of the radical-anion (XXXII) (*a*) and its thallium salt (*b*) in toluene at 20 °C.[49]

When tetrafluorosilane interacts with 3,6-di-t-butyl-1,2-dihydroxybenzene, the EPR spectrum of the radical-anion (XXXII) is also recorded. Under the conditions indicated, the formation of large amounts of HF is apparently inevitable, which displaces the above equilibrium towards (XXXII):



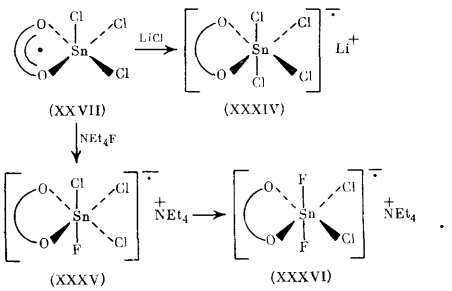
When thallium semiquinolate interacts with tetrafluorosilane, the corresponding thallium salt (XXXIII) is formed and the splitting due to the ^{203}Tl and ^{205}Tl nuclei (a_{Tl} = 2.1 G) is recorded (Fig. 13*b*):



(XXXIII)

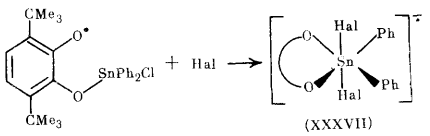
The 3,6-di-t-butyltrifluorostannyl-*o*-semiquinone complex forms analogous salts in moist toluene as a result of the formation of HF during the reaction. Hyperfine coupling with the four nuclei, equivalent in pairs and having a spin of 1/2, is then recorded, two signals referring to the ring protons (a_H = 3.8 G) and the other two to the ^{19}F nuclei located outside the nodal plane of the free radical ligand (a_F = 4.2 G).

Tin-containing complexes of the radical-anion type [the complexes (XXXIV), (XXXV), and (XXXVI)] have been obtained also by the addition of lithium halides in the presence of crown-ether and tetraethylammonium to a toluene solution of the complex (XXVII):



(XXVII) (XXXIV) (XXXV) (XXXVI)

Hyperfine coupling with the two equivalent ring protons of the *o*-semiquinone ligands, the halogen nuclei located outside the nodal plane, and the ^{117}Sn and ^{119}Sn nuclei is detected in the EPR spectra of the complexes (XXXIV) to (XXXVI). Complexes of an analogous type [the complexes (XXXVII)] arise also when the 3,6-di-t-butyldiphenylchlorostannyloxyphenoxy-radical, where the coordination number is in essence four, is treated with the same salts[51]:



(XXXVII)

where Hal = Cl^- (XXXVIIa) or F^- (XXXVIIb).

Table 6 lists the spectroscopic parameters of the radical-anionic complexes obtained. In the instance indicated above, the transformation of a typical phenoxy-radical into an octahedral chelate complex can be seen. This transition as well as the equalisation of the lengths of the Sn–O bonds apparently take place as a result of the intramolecular charge transfer to the univalent oxygen atom from the central atom which is electronically saturated by the additional halide anion. After treating the 3,6-di-t-butyl-2-triphenylstannyloxyphenoxy-radical with salts, we were unable to detect the formation of radical-anionic complexes. This shows that the stability of the octahedral radical-anionic complexes is determined by the electron deficit of the central atom, which depends in its turn on the number of halogen atoms bound to it[52].

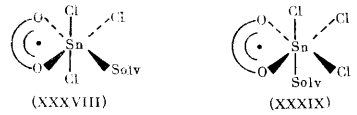
Table 6. The spectroscopic parameters (G) of the radical-anionic complexes of tin with the 3,6-di-t-butyl-1,2-dihydroxybenzene ligands in toluene at 20 °C.[51]

Complex	$a_{H(1)=a_{H(5)}}$	$a_{^{35,37}Cl}$	a_F
(XXXIV)	3.6	0.6 (2)	—
(XXXV)	3.7	0.6 (1)	4.1 (1)
(XXXVI)	3.7	—	4.0 (2)
(XXXVIIa)	3.7	0.6 (2)	—
(XXXVIIb)	3.7	—	4.0 (2)

Note: $a_{^{117,119}Sn}$ = 6.0 G for all the complexes indicated; the number of chlorine or fluorine atoms respectively is indicated in brackets.

Electron-donating molecules can also form complexes with pentacoordinate compounds of Group IV elements. It follows from the analysis of their EPR spectra that the coordinated molecule can be located either in the plane of

the *o*-semiquinone ligand or outside it. Thus the complex (XXVII) can give rise to one of the structures indicated below depending on the nature of the ligand entering it[44]:

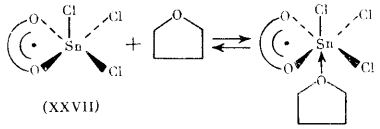


(XXXVIII) (XXXIX)

Solv = CH_3COCH_3, CH_3CN, DMF Solv = $P(O)R_3$, THF

Hyperfine coupling with two $^{35}Cl(^{37}Cl)$nuclei (apart from the hyperfine coupling with the equivalent ring protons) is detected in the spectra of the complexes (XXXVIII) and hyperfine coupling with a single $^{35}Cl(^{37}Cl)$nucleus is detected in the spectra of structure (XXXIX). For complexes where a phosphate molecule is coordinated to the central atom, additional splitting by the ^{31}P nucleus, amounting to approximately 0.2–0.4 G, is detected, which confirms the coordination of the phosphate outside the plane of the free-radical ligand. These complexes are extremely stable and the form of the spectra does not change over a wide temperature range (up to 100 °C).

A complex of type (XXXIX) with THF, which is in equilibrium with the initial complex (XXVII) and free THF, is an exception:



(XXVII)

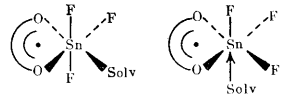
The spectra of the free complex (XXVII) and the complex solvated by THF molecules have the same hyperfine structure, but their *g*-factors differ somewhat. Analysis of the line intensities of both species made it possible to estimate the thermodynamic parameters of the above equilibrium: K_p(20 °C) = 0.23 litre mol^{-1}, ΔH = 4.1 kcal mol^{-1}, and ΔS = −14 e.u.

Table 7. The spectroscopic parameters (G) of the 3,6-di-t-butyl-*o*-semiquinone complex containing the trifluorostannyl group in various solvents at 20 °C.[56]

Solvent	α	$a_{H(4)}$	$a_{H(5)}$	a_F	a_F	$a_{^{117}Sn}$	$a_{^{119}Sn}$
Diethyl ether	0.6	4.1	3.6	4.1	4.1	13.4	14.0
		3.9	3.9	4.4	—	11.9	12.3
THF	0.3	4.1	3.6	4.1	4.1	12.8	13.5
		3.9	3.9	4.4	—	12.5	13.2
Acetone	0.1	4.2	3.7	4.2	4.2	13.2	13.8
		3.9	3.9	4.6	—	14.2	14.8
Acetonitrile	0.03	4.1	3.6	4.1	4.1	13.0	13.4
		3.9	3.9	4.6	—	13.2	13.7
Ethanol	0.3	3.8	3.8	4.4	4.1	12.5	12.5
		3.8	3.8	4.7	—	12.8	12.8

Note: the spectroscopic parameters of the complexes (XXXVIIIa) and (XXXIXa) are quoted for each solvent in the upper and lower row respectively; α is the ratio of the mole fractions of the complexes (XXXIXa) and (XXXVIIIa).

The simultaneous existence of complexes of types (XXXVIII) and (XXXIX) has been detected in the EPR spectra of trifluorostannyl complexes with the 3,6-di-t-butyl-*o*-semiquinone ligand in polar solvents. The spectroscopic parameters of these complexes are presented in Table 7, which also lists the ratios of the mole fractions of these forms: α = [(XXXVIII)]/[(XXXIX)].



(XXXVIIIa) (XXXIXa)

The non-equivalence of the ring protons in the form (XXXVIIIa) is due to the slight distortion of the octahedral structure. It is noteworthy that, for measurements in ethanol, the spectroscopic parameters of the form (XXXVIIIa) indicate the absence of distortion of the octahedral configuration. The relative line intensities of the EPR spectra assigned to these forms are independent of temperature, which is apparently associated with the similar thermodynamic stabilities of the two forms.

The molecular octahedral complex formed following the addition of acetylacetone to a toluene solution of the radical (XXIX) (acetylacetone : toluene = 1 : 1), is of interest. The fluorine is substituted in this instance by the acetylacetonate ligand which, being bidentate, occupies two coordination sites in the sphere of the central silicon atom, which leads to the formation of the complex (XL) whose EPR spectrum and structure are illustrated in Fig. 14.

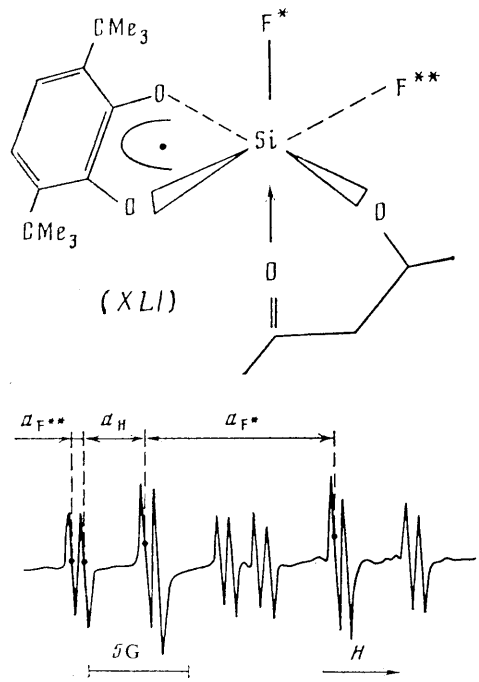
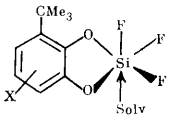


Figure 14. EPR spectrum and structure of the complex (XL) (toluene : acetylacetone = 1 : 1) at 20 °C.[56]

The interaction of SiF_4 with substituted *o*-quinones in solvating solvents—THF, dimethoxyethane (DME), and acetonitrile—yielded *o*-semiquinone complexes whose spectroscopic parameters (Table 8) correspond to an octahedral configuration in which one site outside the plane

of the free-radical ligand is occupied by the solvent molecule (Solv):[50]



(XLI)-(XLIII)

where X = 6-t-butyl (XLI), 5-t-butyl (XLII), or 5-trityl (XLIII). The unexpectedly high constants for hyperfine coupling with the ^{19}F nuclei located in the vicinity of the nodal plane of the free-radical ligand in the complexes (XLII) and (XLIII) are apparently caused by the distortion of the octahedral structure towards a trigonal pyramid as a result of the low symmetry of the *o*-semiquinone ligands.

Table 8. The spectroscopic parameters (G) of the radicals (XLI)–(XLIII) in tetrahydrofuran at −70 °C.[53]

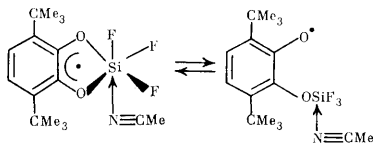
Radical	$a_{H(4)}$	$a_{H(5)}$	a_F	$a_{F'}$
(XLI)	4.1	4.1	0.72 (2)	9.4 (1)
(XLII)	—	4.0	5.50 (2)	9.0 (1)
(XLIII)	—	4.0	5.40 (2)	9.4 (1)

Note: a_F and $a_{F'}$ are the constants for the hyperfine coupling with the fluorine nuclei near and outside the nodal plane of the free-radical ligand. The number of fluorine atoms is indicated in brackets. The constant for the hyperfine coupling with the protons of the t-butyl group in (XLII) is $a_H = 0.5$ G.

The evolution of the EPR spectra of the complex (XLI) as a function of temperature corresponds to the hindered rotation of the trifluorosilyl group relative to the plane of the *o*-semiquinone ligand (Fig. 15): at −70 °C hyperfine coupling with three non-equivalent ^{19}F nuclei is detected, while above 30 °C all three ^{19}F nuclei become equivalent ($a_F = 3.2$ G).[53] Analysis of the line widths in the spectra corresponding to slow exchange made it possible to estimate the rotation frequencies of the SiF_3 group:

$$\nu_{rot}(s^{-1}) = 7\cdot10^{13}\exp[-(6200\pm1000)/RT];\ \nu_{rot}(20^\circ C) = 1.7\cdot10^{9}\ s^{-1}.$$

The mechanism of the hindered rotation can be intermolecular in this instance due to the decomposition of the complex (XLI) and the formation of the complex (XXIX). In the subsequent coordination, a THF molecule can add from the other side, whereupon the relative disposition of the fluorine atoms and the THF molecule can be different. One cannot rule out the possibility that the ligand exchange can be synchronous, i.e. can proceed without the formation of the complex (XXIX). An analogous spectral pattern has been recorded in DME. The spectral changes in acetonitrile at low temperatures (up to 0 °C) also correspond to the hindered rotation of the SiF_3 group. Above 0 °C, the chelate ring opens and the corresponding phenoxy-radical with the trifluorosiloxy-group in the *o*-position is formed. The ring protons then become non-equivalent [$a_{H(4)}$ = 4.0 G, $a_{H(5)}$ = 2.6 G]; on the other hand, the constants for the hyperfine coupling with the ^{19}F nuclei are equalised and greatly diminish ($a_F = 1.7$ G); furthermore, an additional splitting by the ^{14}N nucleus ($a_N = 4.0$ G) of the solvent molecule is detected:



(XLIV) (XLV)

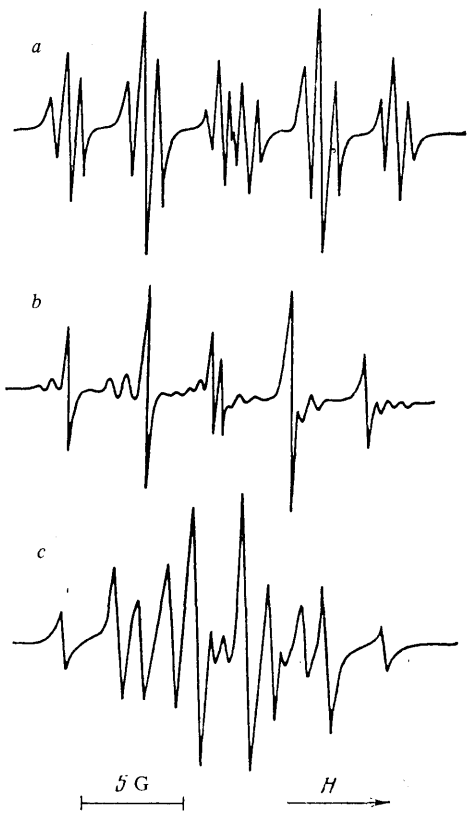
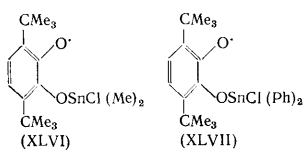


Figure 15. EPR spectra of the complex (XLI) in THF at different temperatures (°C): *a*) −70; *b*) −30; *c*) 30.[53]

The chelate complex (XLIV) can be converted into the phenoxy-radical (XLV) also when the electronegativity of the substituents at the central atom is reduced. Thus, after the replacement of two chlorine atoms in the complex (XXVII) by methyl or phenyl substituents, the chelate complex is converted into the phenoxy-radicals (XLVI) and (XLVII) respectively:



(XLVI) (XLVII)

* *

*

The examples presented show that the application of the EPR and electronic absorption spectroscopic methods to the study of variable-valence metal complexes of *o*-quinones makes it possible to establish the electronic structure of the complexes and to elucidate the wide variety of electronic configurations permitted by the nature of the *o*-benzoquinone ligands.

Analysis of a large number of experimental constants for hyperfine coupling with the magnetic nuclei forming part of the composition of the ligands in the paramagnetic *o*-quinone complexes of Group IV elements permits a conclusion concerning the geometrical structures of the complexes and about the alteration of the latter following the coordination of new ligands, which is of general interest for the chemistry of coordination compounds.

REFERENCES

1. W.R.Harris, C.J.Carrano, and K.N.Raymond, J.Amer.Chem.Soc., 1979, **101**, 2213.
2. A.Avdeev, S.R.Sofen, T.L.Bregante, and K.N.Raymond, J.Amer.Chem.Soc., 1978, **100**, 5362.
3. V.N.Petrov, "Fiziologiya i Patologiya Obmena Zheleza" (The Physiology and Pathology of Iron Metabolism), Izd.Nauka, Leningrad, 1982, p.150.
4. C.G.Pierpont and R.M.Buchanan, Coord.Chem. Rev., 1981, **38**, 45.
5. W.R.Harris and K.N.Raymond, J.Amer.Chem.Soc., 1979, **101**, 6534.
6. L.A.Nikonova, A.G.Ovcharenko, O.N.Efimov, V.A.Avilov, and A.E.Shilov, Kinetika i Kataliz, 1972, **13**, 1602.
7. J.P.Wilshire and D.T.Sawyer, J.Amer.Chem.Soc., 1978, **100**, 3972.
8. D.G.Brown, J.T.Reinprecht, and G.C.Vogel, Inorg. Nuclear Chem.Letters, 1976, **12**, 399.
9. G.A.Razuvaev, V.K.Cherkasov, and G.A.Abakumov, J.Organometal.Chem., 1978, **160**, 361.
10. R.M.Buchanan and C.G.Pierpont, J.Amer.Chem.Soc., 1980, **102**, 4951.
11. V.A.Muraev, V.K.Cherkasov, G.A.Abakumov, and G.A.Razuvaev, Dokl.Akad.Nauk SSSR, 1977, **236**, 620.
12. G.A.Razuvaev, K.G.Shal'nova, L.G.Abakumova, and G.A.Abakumov, Izv.Akad.Nauk SSSR, Ser.Khim., 1977, 1642.
13. I.A.Teplova, K.G.Shal'nova, G.A.Abakumov, and G.A.Razuvaev, Dokl.Akad.Nauk SSSR, 1977, **235**, 1323.
14. A.V.Lobanov, G.A.Abakumov, and G.A.Razuvaev, Dokl.Akad.Nauk SSSR, 1977, **235**, 824.
15. M.S.Wrighton and D.S.Ginley, J.Amer.Chem.Soc., 1975, **97**, 2065.
16. G.A.Bowmaker and G.K.Campbell, Austral.J.Chem., 1979, **32**, 1897.
17. T.Foster, K.S.Chen, and I.K.S.Wan, J.Organometal. Chem., 1980, **184**, 113.
18. A.Alberty and C.M.Camagi, J.Organometal.Chem., 1978, **161**, C-63.
19. L.Pasimeni, P.L.Zanoat, and C.Corvaya, Inorg.Chim. Acta, 1979, **37**, 241.
20. S.P.Solodovnikov, K.Sarbasov, B.L.Tumanskii, N.N.Bubnov, A.I.Prokof'ev, and M.I.Kabachnik, Dokl.Akad.Nauk SSSR, 1982, **265**, 893.
21. K.M.N.Gerber and J.K.S.Wan, J.Amer.Chem.Soc., 1981, **103**, 2101.
22. B.L.Tumanskii, K.Sarbasov, S.P.Solodovnikov, N.N.Bubnov, A.I.Prokof'ev, and M.I.Kabachnik, Dokl.Akad.Nauk SSSR, 1981, **259**, 611.
23. K.Sarbasov, B.L.Tumanskii, S.P.Solodovnikov, N.N.Bubnov, A.I.Prokof'ev, and M.I.Kabachnik, Izv.Akad.Nauk SSSR, Ser.Khim., 1892, 550.
24. P.Hobra, P.Carsky, and R.Zahradnik, Coll.Czech. Chem.Comm., 1973, **38**, 641.
25. I.B.Afanas'ev and N.I.Polozova, Zhur.Org.Khim., 1978, **14**, 1013.
26. E.J.Nanni, M.D.Stallings, and D.T.Sawyer, J.Amer.Chem.Soc., 1980, **102**, 4481.
27. A.I.Prokof'ev, S.P.Solodovnikov, I.S.Belostotskaya, and V.V.Ershov, Izv.Akad.Nauk SSSR, Ser.Khim., 1974, 199.
28. D.Weir and J.K.S.Wan, J.Organometal.Chem., 1981, **220**, 323.
29. M.S.Wrighton, Chem.Rev., 1974, **74**, 401.
30. K.Sarbasov, Candidate's Thesis in Chemical Sciences, Institute of Organoelemental Compounds, USSR Academy of Sciences, Moscow, 1983.
31. R.M.Buchanan, L.Kessel, H.H.Downs, C.G.Pierpont, and D.N.Hendrickson, J.Amer.Chem.Soc., 1978, **100**, 7984.
32. R.M.Buchanan and C.G.Pierpont, Inorg.Chem., 1979, **18**, 3439.
33. S.P.Solodovnikov, A.N.Nesmeyanov, N.A.Volkenau, N.A.Sinitsyna, and L.S.Kotova, J.Organometal.Chem., 1979, **182**, 169.
34. A.Abragam and B.Bleaney, "Electron Paramagnetic Resonance of Transition Metal Ions" (Translated into Russian), Izd.Mir, Moscow, 1972, Vol.1, p.530.
35. I.N.Marov and N.A.Kostromina, "EPR i YaMR v Khimii Koordinatsionnykh Soedinenii" (EPR and NMR in the Chemistry of Coordination Compounds), Izd. Nauka, Moscow, 1979, pp.46, 115.
36. R.M.Buchanan and C.G.Pierpont, Inorg.Chem., 1979, **18**, 1616.
37. C.G.Pierpont and H.H.Downs, J.Amer.Chem.Soc., 1975, **97**, 2123.
38. C.G.Pierpont and R.M.Buchanan, J.Amer.Chem. Soc., 1975, **97**, 6450.
39. S.R.Sofen, D.C.Wate, S.R.Cooper and K.N.Raymond, Inorg.Chem., 1979, **18**, 234.
40. S.S.Isied, G.Kuo, and K.N.Raymond, J.Amer.Chem. Soc., 1976, **98**, 1763.
41. H.H.Downs, R.M.Buchanan, and C.G.Pierpont, Inorg.Chem., 1979, **18**, 1736.
42. K.Sarbasov, B.L.Tumanskii, S.P.Solodovnikov, N.N.Bubnov, A.I.Prokof'ev, M.A.Kurykin, and M.I.Kabachnik, Khim.Fiz., 1982, 1570.
43. K.Sarbasov, S.P.Solodovnikov, B.L.Tumanskii, N.N.Bubnov, and A.I.Prokof'ev, Izv.Akad.Nauk SSSR, Ser.Khim., 1982, 1509.
44. A.I.Prokof'ev, Z.K.Kasymbekova, N.N.Bubnov, S.P.Solodovnikov, and M.I.Kabachnik, Izv.Akad. Nauk SSSR, Ser.Khim., 1982, 1275.
45. R.Luckenbach, "Dynamic Stereochemistry of Pentacoordinated Phosphorus and Related Elements", Georg.Thieme Publisher, Stuttgart, 1973.
46. R.Sarma, F.Ramirez, I.Ugi, and D.Marquarding, Angew.Chem., Int.Ed., 1973, **12**, 91.
47. A.I.Prokof'ev, S.I.Pombrik, Z.K.Kasymbekova, N.N.Bubnov, S.P.Solodovnikov, D.N.Kravtsov, and M.I.Kabachnik, Izv.Akad.Nauk SSSR, Ser. Khim., 1982, 540.
48. A.J.Collussi, J.R.Morton, and K.F.Preston, J.Phys.Chem., 1975, **79**, 651.

49. A.K.Chekalov, A.I.Prokof'ev, N.N.Bubnov, S.P.Solodovnikov, A.A.Zhdanov, and M.I.Kabachnik, Dokl.Akad.Nauk SSSR, 1983, **262**, 622.
50. A.K.Chekalov, A.I.Prokof'ev, N.N.Bubnov, S.P.Solodovnikov, A.A.Zhdanov, and M.I.Kabachnik, Izv.Akad.Nauk SSSR, Ser.Khim., 1983, 1037.
51. Z.K.Kasymbekova, A.I.Prokof'ev, N.N.Bubnov, S.P.Solodovnikov, and M.I.Kabachnik, Dokl.Akad. Nauk SSSR, 1982, **263**, 352.
52. J.J.Lagowski, "Modern Inorganic Chemistry", Marcel Dekker, New York, 1973, p.375.
53. A.K.Chekalov, A.I.Prokof'ev, N.N.Bubnov, S.P.Solodovnikov, A.A.Zhdanov, and M.I.Kabachnik, Izv.Akad.Nauk SSSR, Ser.Khim., 1983, 1184.
54. K.Sarbasov, B.L.Tumanskii, S.P.Solodovnikov, N.N.Bubnov, and A.I.Prokof'ev, Izv.Akad.Nauk SSSR, Ser.Khim., 1983, 2236.
55. S.P.Solodovnikov, K.Sarbasov, B.L.Tumanskii, A.I.Prokof'ev, V.B.Vol'eva, N.N.Bubnov, and M.I.Kabachnik, Izv.Akad.Nauk SSSR, Ser.Khim. (In the Press).
56. A.I.Prokof'ev, Z.K.Kasymbekova, N.N.Bubnov, S.P.Solodovnikov, M.E.Ignatov, E.G.Il'in, and M.I.Kabachnik, Izv.Akad.Nauk SSSR, Ser.Khim. (In the Press).

Nesmeyanov Institute of Organoelemental Compounds, USSR Academy of Sciences, Moscow